

Renormalization Group for Strongly Coupled Maps

Anaël Lemaître^{1,2} and Hugues Chaté^{1,2}

Received November 6, 1998

Systems of strongly coupled chaotic maps generically exhibit collective behavior emerging out of extensive chaos. We show how the well-known renormalization group (RG) of unimodal maps can be extended to the coupled systems, and in particular to coupled map lattices (CMLs) with local diffusive coupling. The RG relation derived for CMLs is nonperturbative, i.e., not restricted to a particular class of configurations nor to some vanishingly small region of parameter space. After defining the strong-coupling limit in which the RG applies to almost all asymptotic solutions, we first present the simple case of coupled tent maps. We then turn to the general case of unimodal maps coupled by diffusive coupling operators satisfying basic properties, extending the formal approach developed by Collet and Eckmann for single maps. We finally discuss and illustrate the general consequences of the RG: CMLs are shown to share universal properties in the space-continuous limit which emerges naturally as the group is iterated. We prove that the scaling properties of the local map carry to the coupled systems, with an additional scaling factor of length scales implied by the synchronous updating of these dynamical systems. This explains various scaling laws and self-similar features previously observed numerically.

KEY WORDS: Coupled map lattice; nontrivial collective behavior; renormalization group; spatiotemporal chaos.

1. INTRODUCTION

Renormalization group (RG) ideas have been instrumental in unveiling the universal features of the cascades of bifurcations of nonlinear dynamical systems with few degrees of freedom.⁽²⁾ Simple maps of the real interval such as the logistic map have been the models of choice on which most

¹ LadHyX, Laboratoire d'Hydrodynamique, École Polytechnique, 91128 Palaiseau, France.

² CEA, Service de Physique de l'État Condensé, Centre d'Études de Saclay, 91191 Gif-sur-Yvette, France.

theoretical advances were made.^(3, 1, 4, 6) These results have contributed greatly to our understanding of (temporally) chaotic systems.

Our current understanding of *spatiotemporal chaos* is, however, much less advanced, and no similarly general framework is available. As a matter of fact, even the term spatiotemporal chaos is somewhat ill-defined, loosely referring to situations where the basic equations cannot be legitimately reduced to the interaction of a few modes. Of all models of spatiotemporal chaos, coupled map lattices (CMLs) are among the most attractive. These discrete-time discrete-space dynamical systems in which maps, arranged at the nodes of a lattice, interact locally can be seen as the direct correspondents, at the spatiotemporal level, of the simple maps of the interval mentioned above. Existing literature on CMLs tend to be overwhelmingly descriptive, stressing the ability of these models to mimic nature, but lacking unifying, structuring results.⁽⁷⁾ In particular, there is not, so far, any notion of universality akin to that at work within low-dimensional dynamical systems.

In this context it has appeared natural to some researchers to try to extend single-map RG to CMLs, in the hope of uncovering some universal features of these systems, and more generally, of spatiotemporal chaos. These works are, however, restricted to perturbative treatments around the accumulation points of bifurcation cascades of the local map and usually consider the limit of weak coupling between maps for configurations limited to small deviations from spatially-homogeneous solutions in one or two space dimensions.^(8, 9) One notable exception is the numerical work of van de Water and Bohr,⁽¹⁰⁾ who showed numerically that many quantities of interest do exhibit scaling properties related to those of the local map, even for rather large values of the coupling.

Recently, we introduced a non-perturbative renormalization group approach to CMLs with linear diffusive coupling which translates to the spatiotemporal level the universal features of the local maps involved.⁽¹¹⁾ We showed that, under broad conditions, the bifurcation diagrams of CMLs present the same self-similarity as that of their local maps, with the same coupling-independent accumulation point, around which lengthscales diverge with a universal scaling related to the diffusive coupling. Here, we give a more comprehensive exposition of these results, following in particular the approach of Collet and Eckmann of the RG for simple maps.⁽¹⁾

The paper is organized as follows. In Section 2, we define the general CMLs we study, which consist of identical, chaotic, unimodal, local maps coupled by a local “diffusive” coupling operator. We then present a short description of their collective dynamics in the limit of strong coupling between maps, which are the regimes where our RG approach is most important since it then applies to almost all asymptotic solutions. This is

followed by the introduction of the continuous-space limit of these CMLs, which plays a major role in the RG treatment.

Section 3 is devoted to a precise definition and a quantitative estimate of the strong-coupling limit mentioned above. Various degrees of collective dynamics are defined, and their relationship to the band structure of the local chaos explained.

Our extension of RG methods to CMLs is first presented in Section 4 for the case of coupled tent maps, where the RG is exact and explicit. The consequences of these results on various dynamical properties are also discussed.

In Section 5, we treat the case of coupled general unimodal maps. The approach of Collet and Eckmann is formally extended to CMLs, and approximations of their RG are introduced.

Section 6 is a conclusion where we summarize our results and discuss some general issues related to our findings.

2. COLLECTIVE DYNAMICS

We consider the discrete-time evolution of an infinite ensemble of (real) variables $\mathbf{X} = (\mathbf{X}_{\vec{r}})_{\vec{r} \in \mathcal{L}}$ for some index set \mathcal{L} . In the following, \mathcal{L} will usually represent a regular lattice, but the case of globally-coupled maps will also be discussed. Each *local* variable takes its value on an interval I while the whole configuration \mathbf{X} lies in the phase space $\mathbf{I} = I^{\mathcal{L}}$. The instantaneous configuration \mathbf{X}^t is updated synchronously by

$$\mathbf{X}^{t+1} = \Delta \circ \mathbf{S}(\mathbf{X}^t) \quad (1)$$

where \mathbf{S} transforms each variable $\mathbf{X}_{\vec{r}}^t$ by a non-linear local map S , and Δ is a linear coupling operator.³ Following classic works on single maps, we consider one-parameter families of non-linear local maps. Without loss of generality, such maps can be written under the form

$$S_{\mu}(X) = 1 - \mu |X|^{1+\varepsilon} \quad \text{with } \mu \in [0, 2] \quad \text{and } \varepsilon \geq 0 \quad (2)$$

which leaves the interval $I = [-1, 1]$ invariant. We will in particular consider, in the following, the tent ($\varepsilon = 0$) and the logistic ($\varepsilon = 1$) maps.

Such dynamical systems exhibit a rich phenomenology rooted in the opposition between the coupling, which drives the local variables towards complete synchronization, and the non-linearity of the map, which may

³ This definition excludes the case of the so-called ‘‘inertial coupling’’ (see, e.g., ref. 7) where the coupling operator involves $\mathbf{S}(\mathbf{X}^t)$ and \mathbf{X}^t itself.

produce chaos. The macroscopic behavior of such systems can be characterized by the evolution in time of \mathcal{L} -averaged quantities like the mean $M^t = \langle \mathbf{X}_{\bar{r}}^t \rangle$, higher-order moments, multi-point correlations, etc. In particular, single-point moments $\langle (\mathbf{X}_{\bar{r}}^t)^k \rangle$ of all orders are contained in the instantaneous distribution (pdf) of local values, p^t . The collective dynamics can be related to emerging mesoscopic structures—formation of clusters, synchronization—and to the microscopic trajectories of local variables.

2.1. Coupled Map Lattices

2.1.1. Diffusive Coupling: General Properties. In the case of coupled map lattices, the local variables $\mathbf{X}_{\bar{r}}$ can be chosen to lie at the nodes of a d -dimensional hypercubic lattice: $\mathcal{L} = \mathbb{Z}^d$, and Δ to be a diffusive coupling operator. In the following, we consider operators Δ which verify some basic properties:⁽⁸⁾

1. Linearity, homogeneity and symmetry, which allow to write,

$$[\Delta(\mathbf{X})]_{\bar{r}_1} = \int \mathcal{D}(\bar{r}_1 - \bar{r}_2) \mathbf{X}_{\bar{r}_2} d\bar{r}_2$$

where the kernel $\mathcal{D}(\bar{r}_1 - \bar{r}_2)$ only depends on the vector difference between an image site \bar{r}_1 and an antecedent \bar{r}_2 ; spatial symmetry, $\mathcal{D}(\bar{\rho}) = \mathcal{D}(-\bar{\rho})$ guarantees that the spectrum $\tilde{\mathcal{D}}(\vec{k})$ is real.

2. Normalization: $\int \mathcal{D}(\bar{\rho}) d\bar{\rho} = 1$ or, equivalently, $\tilde{\mathcal{D}}(\vec{0}) = 1$, and non-negativity: $\mathcal{D}(\bar{\rho}) \geq 0$. This implies that the spectrum $\tilde{\mathcal{D}}(\vec{k})$ of Δ lies in the unit circle. The coupling operator has only one eigenvalue equal to 1 corresponding to the configurations where all sites are synchronized; the others are smaller than one, and therefore all volumes in phase space shrink to the line \mathbf{I}_{syn} of synchronized states when Δ is applied repeatedly.

3. Locality: $\int \bar{\rho}^2 \mathcal{D}(\bar{\rho}) d\bar{\rho} = \lambda_0^2 < \infty$ is a diffusion constant, and the *coupling length* λ_0 defines the range of the coupling. It is proportional to the lattice mesh size $\|\vec{e}\|$ (usually taken to 1): $\lambda_0 = c_0 \|\vec{e}\|$.

These properties lead to the following form of the spectrum in the region of small wavenumbers:

$$\tilde{\mathcal{D}}(\vec{k}) = 1 - \frac{\lambda_0^2}{2} k^2 + \dots \quad (3)$$

The large-scale dynamics of coupled systems is expected to depend essentially on the coupling range λ_0 and not on the particular definition of the coupling operator.

For numerical convenience, the diffusive coupling is usually taken to be the so-called *forward* coupling to nearest-neighbors:

$$[\Delta_g(\mathbf{X})]_{\vec{r}} = (1 - 2dg) \mathbf{X}_{\vec{r}} + g \sum_{\vec{e} \in \mathcal{V}} \mathbf{X}_{\vec{r} + \vec{e}} \quad (4)$$

where g is the *coupling strength*, and \mathcal{V} denotes the set of the $2d$ nearest-neighbors of site $\vec{0}$. This operator verifies the properties (1)–(3) with $\lambda_0 = \sqrt{2g} \|\vec{e}\|$. Even though we do not consider this possibility in the following, our results also apply to the so-called *backward* coupling, defined implicitly through the relation

$$[\Delta_g(\mathbf{X})]_{\vec{r}} = \mathbf{X}_{\vec{r}} + g \sum_{\vec{e} \in \mathcal{V}} ([\Delta_g(\mathbf{X})]_{\vec{r} + \vec{e}} - [\Delta_g(\mathbf{X})]_{\vec{r}})$$

2.1.2. Lattice Dynamics. Let us now present shortly the behavior displayed during numerical simulations of the system $\Delta_g \circ S_\mu$ where the coupling operator is defined by Eq. (4).

The behavior of the local map S_μ is well-known. Parameter space is divided into two parts. For small values of μ , the only attractors are periodic cycles of period 2^k , while chaotic behavior can be observed for $\mu > \mu_\infty$ (with $\mu_\infty = 1$ for the tent map, and $\mu_\infty = 1.401\dots$ for the logistic map).

In the chaotic region of the local map and for the strong, “democratic”, equal-weight coupling $g = 1/(2d + 1)$, the CMLs defined above display *nontrivial collective behavior* (NTCB):⁽¹²⁾ almost all initial conditions flow towards one of a few attractors which possess a well-defined infinite-size, infinite time limit (see Section 3 below and ref. 13 for a quantitative assessment of this statement). In the asymptotic regime, spatial averages usually display a low-dimensional motion (periodic, quasi-periodic,...) while local trajectories are chaotic. (Chaos is in fact *extensive*, as seen, e.g., from the proportionality of the Kolmogorov–Sinai entropy to the volume of the system.) Figures 1(a) and 2(a) show the bifurcation diagrams of the spatial average $M^t = \langle \mathbf{X}_{\vec{r}}^t \rangle$ for two- and three-dimensional lattices of coupled tent maps. Decreasing μ at fixed g , one observes period-doubling of the collective behavior, reminiscent of the self-similar structure of bands of the local map. The instantaneous distribution p^t is smooth and well-defined in the infinite-size limit and follows the same collective behavior as M^t . These period-doubling macroscopic bifurcations are actually Ising-like phase transitions, and their critical points μ_n^c differ from the band-splitting points $\bar{\mu}_n$ of S_μ .⁽¹⁴⁾

Approaching μ_∞ , it rapidly becomes numerically impossible to resolve the NTCB since prohibitively large lattices as well as increasing numerical

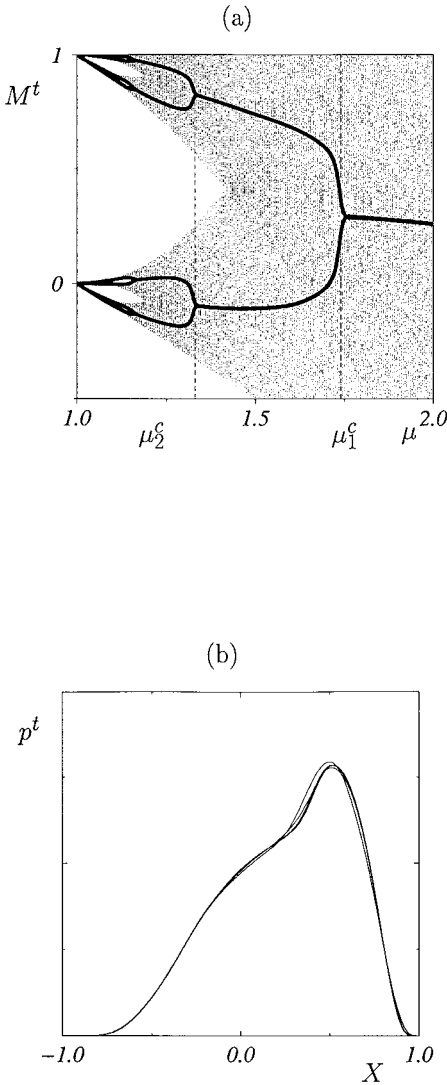


Fig. 1. Democratically-coupled ($g=0.2$) tent maps on a $d=2$ lattice of linear size $L=2048$ with periodic boundary conditions: (a) bifurcation diagram of $M^t = \langle X \rangle^t$ (filled circles) superimposed on that of the local map S_μ (small dots). (b)–(d): Asymptotic (large t) dynamics of the single-site distributions p^t : (b): stationary states at $\mu=2$ for the system $\Delta_g^m \circ S_\mu$ and $1 \leq m \leq 32$: $p^t \rightarrow p_m$. For $m > 1$, the asymptotic distributions cannot be separated on this graph; when m increases, they converge to a universal distribution which is the asymptotic state reached in the continuous limit $\Delta_\lambda^\infty \circ S_\mu$. (c): The existence of this limit distribution is evidenced by the log–log plot of the distance $D^2 = \int dX (p_m - p_{32})^2$ vs m . (d): period-2 collective cycle at $\mu = \bar{\mu}_1$ for $m=1$.

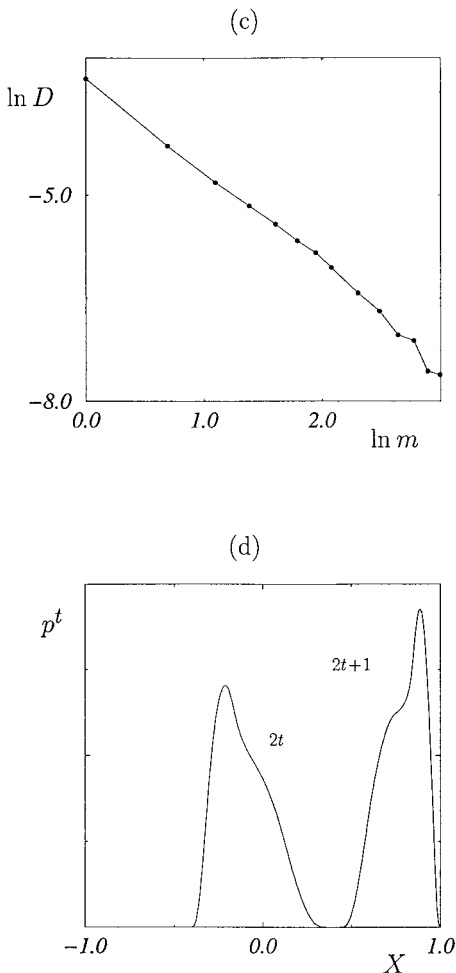


Fig. 1. (Continued)

resolution are then required. In particular, near μ_∞ the uniqueness of the attractor cannot be ascertained, and no evidence of an infinite cascade of phase transitions is available.

Although only periodic motion have been observed in dimensions $d=2$ and 3 (see Figs. 1(a) and 2(a)), more complex NTCB exist for $d>3$. Four-dimensional CMLs display regions of the parameter μ where two periodic attractors coexist (e.g., period-2 and period-4 collective regimes for coupled tent maps). Five-dimensional CMLs display quasi-periodic collective behavior.⁽¹²⁾

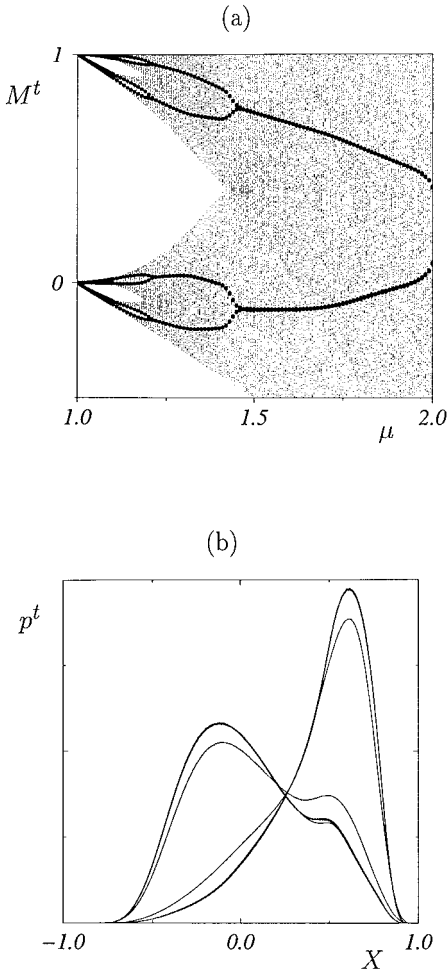


Fig. 2. $d=3$ lattice of democratically-coupled ($g=1/7$) tent maps of linear size $L=128$ with periodic boundary conditions: (a): bifurcation diagram of M^t (filled circles) superimposed on that of the local map (small dots). (b): Asymptotic period-2 collective cycle for the single-site distribution p^t at $\mu=2$ for $1 \leq m \leq 8$. (c): log-log plot of the distance $D^2 = \int dX (p_m - p_8)^2$ vs m . (d): Asymptotic period-4 collective cycle for the single-site distribution p^t at $\mu = \bar{\mu}_1$ for $m=1$.

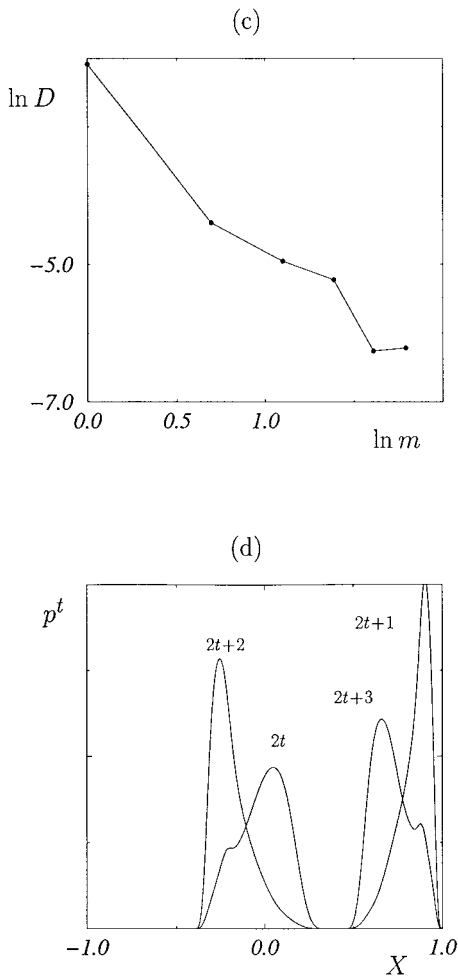


Fig. 2. (Continued)

2.2. Continuous Limit

2.2.1. Iterated Couplings. A straightforward generalization of CMLs of the form $\Delta_g \circ \mathbf{S}_\mu$ consists in applying several times the operator Δ_g after each transformation \mathbf{S}_μ : the evolution operator becomes $\Delta_g^m \circ \mathbf{S}_\mu$ and involves the m -th neighborhood of each site. Although the importance of such systems is not evident at this stage, they play an essential role in the RG (see Section 4).

In the small wavenumber limit, the spectrum of Δ_g^m reads,

$$\tilde{\mathcal{G}}_g^m(\vec{k}) = 1 - \frac{\lambda_0^2 m}{2} k^2 + \dots$$

For large m , the iterated operator Δ_g^m is equivalent to the coupling operator with Gaussian kernel:

$$\Delta_{g \ m \rightarrow \infty}^m \simeq \Delta_\lambda^\infty = \exp\left(\frac{\lambda^2}{2} \nabla^2\right)$$

where $\lambda = \lambda_0 \sqrt{m} = c_0 \sqrt{m} \|\vec{e}\|$ is the typical range of the coupling and $\|\vec{e}\|$ is the lattice mesh size.

The *coupling length* λ fixes the size of small spatial structures, i.e., it characterizes the lengthscale over which the field $\mathbf{X}_{\vec{r}}$ varies: below λ , sites are nearly synchronized. When m increases, these structures spread out, and in the limit $m \rightarrow \infty$ the coupling length diverges *relatively to the lattice mesh size* $\|\vec{e}\|$.

In fact, when observing the collective behavior of such a system, one must consider spatially averaged quantities: this requires to sum over spatial disorder, i.e., over some lengthscale A much larger than λ , the number of independent structures in the system being $(A/\lambda)^d$. This indicates that λ is the relevant lengthscale for macroscopic dynamics and that all length-scales should be considered proportionally to λ and not to the lattice mesh size, which is irrelevant. Taking the limit $m \rightarrow \infty$ while keeping a fixed number of independent “units”, amounts to keep λ fixed while resealing $\|\vec{e}\|$ as:

$$\|\vec{e}\| \propto 1/\sqrt{m} \rightarrow 0$$

This defines the *continuous limit* of coupled map lattices in which a d -dimensional field of variables $\mathbf{X} = (\mathbf{X}_{\vec{r}})_{\vec{r} \in \mathcal{L}}$, $\mathcal{L} = \mathcal{R}^d$, evolves under the discrete-time dynamics $\Delta_\lambda^\infty \circ \mathbf{S}_\mu$. No continuous-time limit is defined for such systems: they constitute a Poincaré-section version of the evolution of spatially extended systems. For the system $\Delta_\lambda^\infty \circ \mathbf{S}_\mu$, the parameter λ plays a trivial role since it is the only length scale which remains after the limit $\|\vec{e}\| \rightarrow 0$ has been taken: changing λ amounts to a mere zoom over space. Therefore, the collective behavior of one-site macroscopic variables like M^t or p^t does not depend on λ , while correlation functions are simply rescaled by a change of λ . Note that the limit reached, Δ_λ^∞ , is “universal”, in the

sense that it is independent of the choice of the operator Δ_g , provided it satisfies properties (1)–(3).

2.2.2. Numerics. Careful numerical investigation of dynamics of the form $\Delta_g^m \circ S_\mu$ has been performed for $d=2$ and 3 lattices of democratically-coupled logistic and tent maps for increasing values of m . In these cases, bifurcation diagrams for any m are not distinguishable from those displayed in Fig. 1 corresponding to the case $m=1$. Asymptotic distributions in the fixed point regime of 2-dimensional lattice of size $L=2048$ at $\mu=2$ are given in Fig. 1: at fixed μ , they quickly converge with increasing m to a well-defined asymptotic pdf, as seen from the estimation of the distances $D(p_1, p_2) = \sqrt{\int (p_1 - p_2)^2}$ (see insert of Fig. 1). In these cases at least, the collective behavior is extremely weakly dependent on the details of the coupling, and the lattice behavior is qualitatively, and, to a large extent, quantitatively, similar to the continuous limit.

In higher dimensions, the comparison of the usual CMLs ($m=1$) with systems with increasing values of m , shows noticeable (quantitative and qualitative) differences. For example, in dimension 4, the coexistence of macroscopic attractors seems to disappear for $m \simeq 8$.⁽¹⁵⁾ However, the numerical estimation of the collective behavior displayed in the continuous limit requires lattices of increasing linear size, consequently out of reach of today's even most powerful computers. The precise evaluation of collective behavior in the continuous limit is therefore impossible.

3. CONDITIONS FOR NONTRIVIAL COLLECTIVE BEHAVIOR

Non-trivial collective behavior, as presented in Section 2.1, is displayed by CMLs for “strong” couplings: it was illustrated with the “democratic” value of the coupling strength, namely, $g = 1/(2d + 1)$, which gives the same weight to all sites in the local neighbourhood.

When the local map is in a band-chaotic regime, all sites of a lattice displaying NTCB eventually lie within the same band at any given time: this is the signature of long-range order emerging from the local dynamics. This property plays an important role in the definition of a RG for CMLs, and it is necessary, at this stage, to clarify the conditions of emergence of NTCB.

In this section, we show that the long range order is the result of a coarsening process between all possible macroscopic phases. We also show that there exists a finite threshold value g_c^* of the coupling strength above which NTCB is reached from almost all initial conditions.

3.1. Bands

3.1.1. Banded Chaos. We first review briefly the phenomenology displayed by unimodal maps. Some of their universal features like the order of occurrence of periods⁽⁵⁾ or the internal similarity⁽⁶⁾ depend only on the existence of a unique maximum and this property is usually referred to as structural universality.

When the parameter μ increases, the map S_μ undergoes a cascade of subharmonic bifurcations. We denote μ_n the value at which the period 2^{n-1} regime becomes unstable and above which the system enters period 2^n . These points accumulate at some critical value μ_∞ where the system enters the chaotic regime. Above this value, the local map displays banded chaos, possibly intermingled with parameter windows of periodic behavior.

At the other end of the inverse cascade, at the value $\bar{\mu}_0 = 2$, trajectories run over the whole interval $I = [-1, 1]$. When μ decreases, asymptotic trajectories run over one band $I_{S_\mu}^0 = [1 - \mu, 1]$, the smallest invariant interval for S_μ . This band splits at the value $\bar{\mu}_1$ into two bands $I_{S_\mu}^{1,0} \ni 0$ and $I_{S_\mu}^{1,1}$ which are nonintersecting invariant intervals for the iterated map $S_\mu^2 = S_\mu \circ S_\mu$, and ergodic components for S_μ :

$$I_{S_\mu}^{1,0} \cap I_{S_\mu}^{1,1} = \emptyset, \quad S_\mu(I_{S_\mu}^{1,0}) \subset I_{S_\mu}^{1,1} \quad \text{and} \quad S_\mu(I_{S_\mu}^{1,1}) \subset I_{S_\mu}^{1,0}$$

Below $\bar{\mu}_1$, and for almost all initial conditions, the system reaches a chaotic asymptotic trajectory which flips between the two bands: if X^t lies in the band $I_{S_\mu}^{1,0}$ at some even time, it will be found in $I_{S_\mu}^{1,0}$ (resp. $I_{S_\mu}^{1,1}$) at all following even (resp. odd) times.

Decreasing μ towards μ_∞ , an inverse cascade of band splitting bifurcations occurs. We denote $\bar{\mu}_n$ the point below which the regime with 2^n bands takes place: for $\mu \in [\mu_\infty, \bar{\mu}_n]$, the iterated map $S_\mu^{2^n}$ admits 2^n ergodic components over which asymptotic trajectories of the variable X^t run periodically. Let us denote $I_{S_\mu}^{n,\sigma}$, $\sigma = 0, \dots, 2^n - 1$ these 2^n bands with the following convention: take the "central" band $I_{S_\mu}^{n,0} \ni 0$, and order the bands such that

$$I_{S_\mu}^{n,\sigma} = S_\mu^\sigma(I_{S_\mu}^{n,0})$$

Therefore, the action of S_μ on these bands amounts to the permutation $\sigma \rightarrow (\sigma + 1)[2^n]$ (modulo 2^n).

It is important to note that the intervals $I_{S_\mu}^{n,\sigma}$ are invariant under the map $S_\mu^{2^n}$ for all $\mu \in [\mu_\infty, \bar{\mu}_n]$ even though, approaching μ_∞ , the system reaches regimes with more and more bands. For example, $I_{S_\mu}^0$ is the stable

interval of S_μ , for all μ , and below $\bar{\mu}_1$, the two bands $I_{S_\mu}^{1,0}$ and $I_{S_\mu}^{1,1}$ are defined and are subsets of $I_{S_\mu}^0$: if $\mu \leq \bar{\mu}_n \leq \bar{\mu}_1$, the map has 2^n bands, but $I_{S_\mu}^{1,0}$ and $I_{S_\mu}^{1,1}$ are still exchanged by S_μ and all even (resp. odd) bands lie on $I_{S_\mu}^{1,0}$ (resp. $I_{S_\mu}^{1,1}$):

$$I_{S_\mu}^{n,2\sigma} \subset I_{S_\mu}^{1,0}, \quad \text{and} \quad I_{S_\mu}^{n,2\sigma+1} \subset I_{S_\mu}^{1,1}$$

3.1.2. Banded States. Let us now consider the evolution of some configuration \mathbf{X}^t under an operator of the form $\Delta_g^m \circ S_\mu$. Whenever $\mu \in [\mu_\infty, \bar{\mu}_n]$, the local map has (at least) 2^n bands: we denote $\mathbf{I}_{S_\mu}^{n,\sigma}$ the set of configurations for which all variables \mathbf{X}_r lie on the band $I_{S_\mu}^{n,\sigma}$:

$$\mathbf{I}_{S_\mu}^{n,\sigma} = (I_{S_\mu}^{n,\sigma})^{\mathcal{L}}$$

S_μ operates a permutation on σ , and since the operator Δ_g^m keeps intervals stable, $\Delta_g^m \circ S_\mu$ operates the same permutation $\sigma \rightarrow (\sigma + 1)[2^n]$: these intervals $\mathbf{I}_{S_\mu}^{n,\sigma}$ constitute generalized bands in the phase space $\mathbf{I} = [-1, 1]^{\mathcal{L}}$.

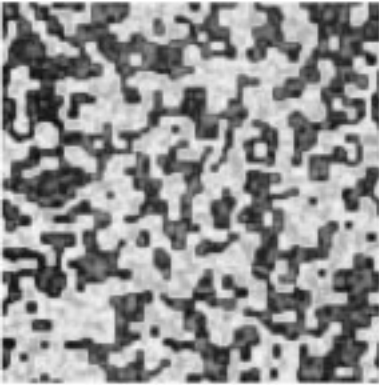
Therefore, if the configuration \mathbf{X}^t falls on some of these intervals at some time, it runs periodically over these 2^n bands at all following times. We call such a state of the system a *banded state of order n* (BS n). The fact that the system is in a BS n does not imply that it displays a period- 2^n macroscopic regime: the actual collective behavior could be of higher (multiple) periodicity, or even quasiperiodic. For example, the $d=3$ lattice of coupled tent maps shown in Fig. 2 displays a period-2 behavior for $\mu = \bar{\mu}_0$, and the two-dimensional lattice displays period-2 just above $\mu = \bar{\mu}_1$: these are banded states of order 0 since the local map has only one band.

3.2. Nontrivial Synchronization

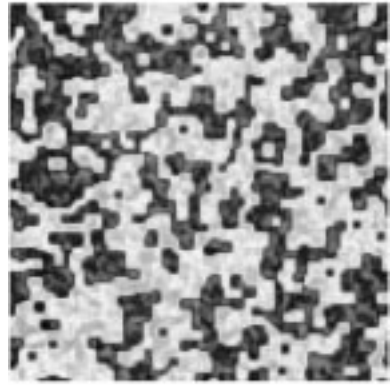
When the local map has several bands, the coupled map system operates a permutation on the bands $\mathbf{I}_{S_\mu}^{n,\sigma}$ in the phase space: if all sites of the lattice lie in the same band at some given time (say $t = t_0$), they run together periodically over the bands of the local map. Suppose now that not the whole lattice, but some region of the lattice $\ell \in \mathcal{L}$ only has all its sites in the same band $I_{S_\mu}^{n,\sigma}$ (with, say $\sigma = 0$) at t_0 while all other variables lie in another band (say $\sigma = 1$). Inside each of these domains, the variables follow a collective regime which resembles a BS at a mesoscopic scale. However, different situations can occur at the boundaries: one domain can invade the other, in which case the system converges towards a BS, or the fronts can be blocked and clusters of different phases can coexist on the same lattice.

These situations are illustrated in Figs. 3–4 using a two-dimensional lattice of coupled tent maps for $\mu = 1.4$, a case in which the local map has two bands. Starting from random initial conditions, mesoscopic regions start flowing towards the two-band attractor: some regions of the lattice try to follow a period-2 evolution with $\sigma = 0$ while the other regions converge

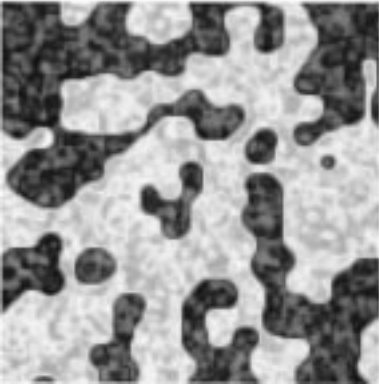
(a)



(b)



(c)



(d)

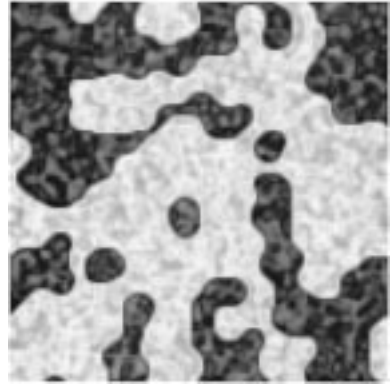


Fig. 3. Snapshot of a 2-dimensional lattice of coupled tent maps of size $N = 128^2$ with periodic boundary conditions and $\mu = 1.4$, $g = 0.08$: (a) after a transient (b) 10000 time steps later. A few small clusters have been eliminated while the largest structures are blocked in the space and do not evolve any longer. Inside a cluster, the dynamics is similar to that of a banded state: the local variables evolve chaotically while the cluster as a whole follows a period-2 regime. (c)–(d) same for $g = 0.1$.

to the same evolution with the phase $\sigma = 1$. During the first time steps of the dynamics, clusters are formed due the indetermination on σ .

For small coupling strengths (see Fig. 3), the boundaries between these domains form walls that the coupling cannot break: the walls are pinned to the lattice and clusters persist in the infinite-time limit. The pinning allows for the co-existence of clusters on the same lattice and all

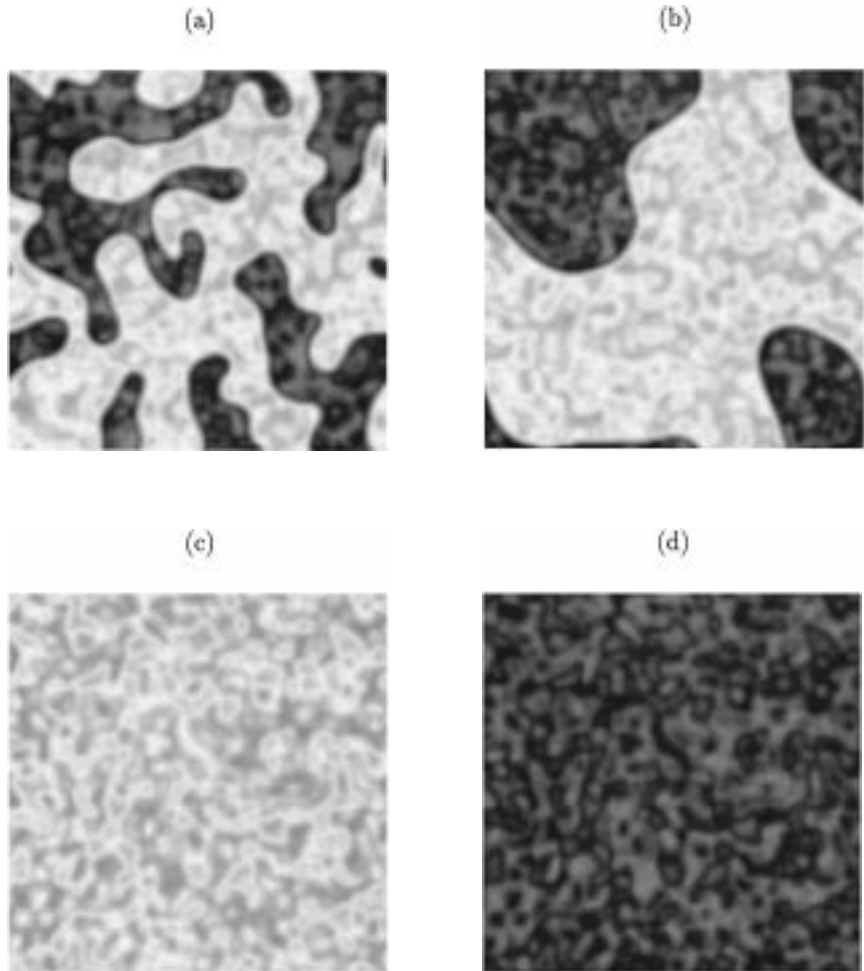


Fig. 4. Snapshot of a 2-dimensional lattice of coupled tent maps of size $N = 128^2$ with periodic boundary conditions and $\mu = 1.4$, $g = 0.2$: (a) after a short transient (b) 1000 time steps later. The fronts between the two phases propagate so that the small structures are eliminated. (c)–(d) 10000 and 10001 time steps later only one phase remains.

the possible patterns correspond to the “ergodic components” of the dynamical system.

For stronger values of the coupling, the domain wall structure is broken as illustrated in Fig. 4 for the same lattice but with $g=0.2$. The comparison of the same lattice at different time-steps show that the smaller clusters are eliminated: except for exceptional initial conditions leading to a flat interface between the two phases, the system converges towards a banded state, and there is a unique attractor for the collective regime.

We call *non-trivial synchronization* (NTS) the property that the system reaches a BS from (almost) all initial conditions. Estimating quantitatively the value of the coupling marking the onset of NTS is a difficult task. We now briefly present how this can be achieved in the simple case of NTS to a BS1. More detailed results will be published elsewhere.⁽¹³⁾

3.3. Estimating the Onset of NTS: Phase Ordering of Coarse-Grained Variables

Take some $\mu \in [\mu_\infty, \bar{\mu}_1]$, to insure that the local map has two bands, and consider first the uncoupled case ($g=0$): each variable \mathbf{X}_f^t evolves independently under the local map S_μ , and its trajectory reaches the asymptotic regime where it flips between the bands $I_{S_\mu}^{1,0}$ and $I_{S_\mu}^{1,1}$. Depending on its initial value \mathbf{X}_f^0 it falls in $I_{S_\mu}^{1,0}$ at even or odd times, and some phase variable at $\sigma_f^t \in \{0, 1\}$ can be associated to each site. For a finite lattice of N sites, $\mathcal{N} = 2^N/2$ different patterns can be obtained, corresponding to different ergodic components for the dynamics of the configuration \mathbf{X}^t in the phase space \mathbf{I} .

The coarse-grained variables σ_f^t are similar to Ising spins and the diffusive coupling operator Δ_g^m plays the role of some ferromagnetic interaction with range $\lambda = \sqrt{2gm} \|\vec{e}\|$. When g increases, sites try to synchronize, and for strong enough coupling, isolated variables jump to the other phase (e.g., σ_f^t surrounded by $\sigma_{f+\vec{e}}^t = 1$). For a given $g > 0$, only clusters with a minimal transverse size survive: a continuous family of asymptotic states can be observed depending on the proportion of clusters in each phase, and the number of ergodic components is expected to scale like $\mathcal{N} \propto \exp(\alpha N)$ with the system size. Coefficient α decreases when g increases. For large values of the coupling, say $g > g_e^1(\mu, m)$, no cluster persists, all sites end up in one of the two phases and a BS1 is reached from almost all initial condition.

The direct estimation of \mathcal{N} is impossible in practice, although one can easily get a flavor of the sequence of bifurcations marking the decrease of α when g is increased.⁽¹⁶⁾ It is, in fact, easier to estimate $g_e^1(\mu, m)$ from the

behavior of the probability of persistence of the coarse-grained variables, as explained now.

The persistence probability is defined as the fraction P^t of phase variables σ_r^t that have not changed their value since $t=0$ (modulo the period, here two, of the local cycle):

$$P^t = P(\forall t' \leq t, \sigma_r^{t'} = \sigma_r^0 + t'[2])$$

We have performed numerical investigations of the behavior of the persistence probability for $\mu \in [\mu_\infty, \bar{\mu}_1]$ and $m \geq 1$ aiming at estimating $g_e^1(\mu, m)$.

Starting from random initial conditions shared between the two bands, if no coupling is applied ($g=0$), $\sigma_r^t = \sigma_r^0 + t[2]$ for all sites, and $P^t = 1$ at all times. For small but non-zero coupling, the synchronization of phase variables with their neighbors is accounted for by a decay of P^t which saturates at some finite asymptotic value characterizing the pinning of different possible clusters. If g is large enough, however, the system converges towards a BS1, and P^t decreases algebraically to zero, similarly to the quench of an Ising model at zero temperature.⁽¹⁷⁾

Such measurements allow for a rough evaluation of $g_e^1(\mu, m)$ as shown in Fig. 5. Better estimates can be obtained by extrapolating the changes in the scaling behavior of P^t observed at large g to $g \rightarrow g_e^1(\mu, m)$.

The value of $g_e^1(\mu, m)$ decreases when $\mu \rightarrow \mu_\infty$: this is expected since in this limit the tendency of the local map to separate trajectories weakens (decrease of the largest Lyapunov of the lattice).⁴ An immediate consequence of this observation is that there exists a maximal value for fixed m ,

$$g_e^1(m) = \max_{\mu} [g_e^1(\mu, m)] = g_e^1(\bar{\mu}_1, m)$$

above which the system governed by $\Delta_g^m \circ S_\mu$ reaches a BS1 for all $\mu \in [\mu_\infty, \bar{\mu}_1]$ and for (almost) all initial conditions.

Similarly, $g_e^1(\mu, m)$ decreases when m increases, because then the coupling is "stronger". Therefore, there exists a maximal value

$$g_e^{1*} = \max_m [g_e^1(m)] = \max_{\mu, m} [g_e^1(\mu, m)] = g_e^1(\bar{\mu}_1, 1)$$

above which a BS1 is reached for all μ and m .

⁴ In fact, in the particular case of coupled tent maps which is illustrated, $g_e^1(\mu, m) \rightarrow 0$ when the parameter μ approaches μ_∞ . This is not surprising since the local map presents marginal stability at $\mu_\infty = 1$: no divergence of nearby trajectories is opposed to even the smallest couplings; however this is only verified by coupled tent maps.

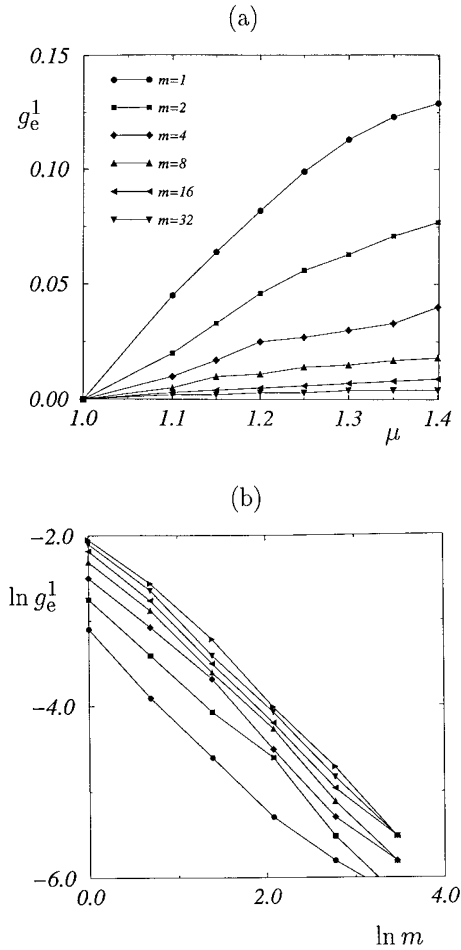


Fig. 5. Values of $g_e^1(\mu, m)$ vs μ (a) and m (b) for 2-dimensional lattices of coupled tent maps ($L = 512$).

As we have seen, in the general case of coupled maps lattices (not necessarily tent maps), taking the limit $m \rightarrow \infty$ with the appropriate rescaling of the lattice mesh size $\|\vec{e}\| \propto 1/\sqrt{m} \rightarrow 0$ yields the continuous limit of the coupling operator. Since the coexistence of phases in the small coupling regime is made possible by the pinning of localized structures on lattice sites as illustrated in Fig. 3, we must expect this effect to disappear in the continuous limit:

$$g_e^1(\mu, m) \xrightarrow{m \rightarrow \infty} 0$$

Finally, in order to study this coarsening process, the “worst” possible situation was considered, where the initial state is chosen so as to insure that the competition between the two macroscopic phases goes on at all times, thus leading to an algebraic decay of persistence. In fact, due the asymmetry between the basins of the two ergodic components of the local map, if the local variables are taken randomly on the interval I at time $t=0$, then one phase dominates the other after a few timesteps. The minority phase is eliminated in finite time at the macroscopic level.

3.4. Banded States When $\mu \rightarrow \mu_\infty$?

Consider $\mu \in [\bar{\mu}_2, \bar{\mu}_1]$: the local map has exactly two bands, and the multistability of the two associated phases disappears at $g_e^1(\mu)$. For g above this value, the system flows towards a BS1 and, asymptotically, all sites lie simultaneously in the same band at any given time. If, however, $\mu \in [\bar{\mu}_3, \bar{\mu}_2]$, the local map has four bands' and local phase variables σ_τ^t take their values in $\{0, 1, 2, 3\}$. The limit value $g_e^1(\mu)$ is still defined, and above it all sites fall into one of the two “meta-bands” $I_{S_\mu}^{1,0}$ or $I_{S_\mu}^{1,1}$: all σ_τ^t are simultaneously either even or odd.

Suppose now that the system is in a BS1, i.e., it flips between the intervals $I_{S_\mu}^{1,0}$ and $I_{S_\mu}^{1,1}$. Pinned clusters can be formed inside these bands, e.g., between the sub-intervals $I_{S_\mu}^{2,0}$ and $I_{S_\mu}^{2,2}$ in $I_{S_\mu}^{1,0}$ and also $I_{S_\mu}^{2,1}$ and $I_{S_\mu}^{2,3}$ in $I_{S_\mu}^{1,1}$: according to this new coarse-graining, an infinite number of attractors can be evidenced again. One can define a limit value of the coupling, $g_e^2(\mu, m)$, above which the system converges towards a BS2 starting from any initial conditions *in* a BS1. Thus, defining

$$g_e^{2*}(\mu, m) = \max(g_e^1(\mu, m), g_e^2(\mu, m))$$

for all $g > g_e^{2*}(\mu, m)$, the system converges towards a BS2 starting from any initial condition.

One can this way define a whole hierarchy of limit coupling values $g_e^n(\mu, m)$ above which a BS n is reached from any initial BS $n-1$. Thus the condition for NTS is defined by

$$g_e^{n*}(\mu, m) = \max_{n' \leq n} g_e^{n'}(\mu, m)$$

above which a BS n is reached from any initial condition.

Understanding NTS in the limit $\mu \rightarrow \mu_\infty$ requires to evaluate all possible $g_e^{n*}(\mu, m)$ in order to establish some general threshold $g_e^*(\mu, m)$ above which NTS is observed at all orders.

It is not clear, at this stage, whether NTS persists in this limit and what occurs at the transition between the periodic $\mu < \mu_\infty$ and chaotic $\mu > \mu_\infty$ regimes of the local map: how does the series g_e^{n*} behaves when $\mu \rightarrow \infty$? In fact, there are (naive) arguments against the existence of an infinite cascade of BS since the local chaos at work among the sites is sometimes represented as some effective noise: chaotic systems with external noise⁽¹⁸⁾ show a truncated (finite) cascade of bifurcation because the refined structure of bands is broken by the noise near μ_∞ . This would correspond to a situation in which, for some given $g > g_e^{1*}$, although a BS1 is reached for all $\mu < \bar{\mu}_1$, the smallest bands could not be separated for μ sufficiently close to μ_∞ . If this appeared to be true, a banded state of high order could not be reached and NTS would not be achieved. The following presentation of RG arguments will clarify these issues.

4. RENORMALIZATION GROUP FOR COUPLED TENT MAPS

The sequences of periodic behavior observed on bifurcation diagrams like those displayed in Figs. 1 and 2 in strong-coupling regimes show similarities with the band structure of the local map. This simple observation raises the question of the existence of some self-similarity within the collective regimes. Since, as mentioned above, NTCB could be lost when approaching μ_∞ , two different questions can be addressed: First, is there some universality displayed by asymptotic banded states, whatever the coupling, if necessary starting from adequate initial conditions? Second, what is the asymptotic regime reached from almost all initial conditions, and is there an infinite cascade of NTCB for sufficiently strong coupling?

The previous section intended to study the second question, but failed to give general answer near μ_∞ , because it requires to evaluate all $g_e^n(\mu, m)$ or at least to provide some upper bound for these thresholds. We now turn to the derivation of a RG equation for coupled maps which applies to all types of banded states and gives a precise answer to the first question. This, in turn, provides a complete description of the phase diagram of coupled map systems in this limit, and therefore answers the second question.

The RG is first derived on the example of coupled tent maps in which case calculation can be carried out exactly while the more general case of unimodal maps is discussed afterwards.

4.1. Known Results for Single Maps

Let us first recall how the RG works in the case of the tent map. In this simple case, the RG stems from the conjugacy between the iterated

map S_μ^2 in the two band regime with the map $S_{\mu'}$ for some other value of the parameter μ' . This RG characterizes the self-similar structure of the dynamical system and provides scaling exponents in the limit $\mu \rightarrow \mu_\infty$ for, e.g., the band-splitting points or the widths of the bands in this limit. One can write the RG in two ways.

Centered RG. For any $\mu > 1$, the second iterate S_μ^2 of the tent map $S_\mu(X) = 1 - \mu |X|$, restricted to the interval $[-1/\mu, 1/\mu]$ reads

$$S_\mu^2|_{[-1/\mu, 1/\mu]}(X) = 1 - \mu + \mu^2 |X|$$

This allows for a change of variable $X' = -X/a$, with $-a = S_\mu(1) = 1 - \mu$: the variable X' is governed by the map $S_{\mu'}$, with $\mu' = \mu^2$ (see Fig. 6).

Whenever $\mu' \leq \bar{\mu}_0$, the map $S_{\mu'}$ leaves the interval $I = [-1, 1]$ invariant. Therefore, X transformed by S_μ^2 cannot escape from the interval $I_{S_\mu}^* = [-a, a]$. The second iterate S_μ^2 of the map restricted to the interval $I_{S_\mu}^*$ is then conjugate to S_{μ^2} via:

$$S_\mu^2|_{I_{S_\mu}^*} = h_{S_\mu}^{-1} \circ S_{\mu^2} \circ h_{S_\mu} \tag{5}$$

with h_{S_μ} the linear transformation $h_{S_\mu}(X) = -X/a$.

In fact, the dynamics defined by $S_{\mu'}$ covers the interval $I_{S_{\mu^2}}^0 \subset I$, and the central band $I_{S_\mu}^{1,0} \subset I_{S_\mu}^*$ is obtained via

$$I_{S_\mu}^{1,0} = h_{S_\mu}^{-1}(I_{S_{\mu^2}}^0)$$

while the condition $\mu' \leq \bar{\mu}_0 = 2$ or $\mu \leq \sqrt{2}$ provides the value of the first band splitting point, $\bar{\mu}_1 = \sqrt{2}$.

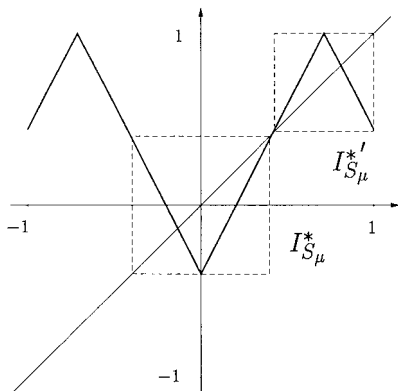


Fig. 6. Iterated tent map S_μ^2 for $\mu = 1.4$, with indication of the intervals $I_{S_\mu}^*$ and $I_{S_\mu}^{*'}$.

Since this relation identifies the iterated map with the tent map itself, the process can be repeated. It shows that S_μ exhibits a self-similar cascade of band-splitting points $\bar{\mu}_n = \sqrt{\bar{\mu}_{n-1}}$ below which regimes with more than 2^n bands are observed. When $n \rightarrow \infty$, the points $\bar{\mu}_n = \sqrt[2^n]{2}$ converge to the fixed point $\mu_\infty = 1$ of $\sqrt{\quad}$ and for large n , the points $\bar{\mu}_n$ converge to μ_∞ like $\bar{\mu}_n - \mu_\infty \sim \delta^{-n}$ which defines the Feigenbaum constant (or the *bifurcation velocity*) (here $\delta = 2$).

Noncentered RG. A conjugacy is also verified for S_μ^2 on the interval $I_{S_\mu}^* = [2/\mu - 1, 1]$. This relation reads,

$$S_\mu^2|_{I_{S_\mu}^*} = h'_{S_\mu}{}^{-1} \circ S_{\mu^2} \circ h'_{S_\mu} \tag{6}$$

for the same parameter $\mu' = \mu^2$ as in the centered version, while $h'_{S_\mu}(X) = (X - 1/\mu)/(1 - 1/\mu)$ and $I_{S_\mu}^* = h'_{S_\mu}{}^{-1}([-1, 1])$. The band $I_{S_\mu}^{1,1}$ is obtained via

$$I_{S_\mu}^{1,1} = h'_{S_\mu}{}^{-1}(I_{S_{\mu^2}}^0)$$

Equation (6) is a non-centered RG equation.

4.2. RG for Coupled Maps

Let us now consider coupled tent map dynamics governed in the general case by an operator of the form $\Delta_g^m \circ S_\mu$. In the spirit of the derivation of a RG for single maps, we are led now to study the iterated operator $(\Delta_g^m \circ S_\mu)^2$ restricted to one of the intervals $I_{S_\mu}^*$ or $I_{S_\mu}^{1,1}$ in the phase space \mathbf{I} . Such an approach requires the single assumption that the system is in a BS1 and concerns all values of the parameter $\mu \in [\mu_\infty, \bar{\mu}_1]$ to insure that the system remains in a BS1 at all times. This situation is encountered either because the coupling is sufficiently strong so that the system flows towards such a BS1 for almost all initial condition— $g \geq g_e^1(\mu, m)$ —, or simply because adequate initial conditions have been chosen, whatever the coupling strength.

4.2.1. Centered RG

Commutation. Take some $\mu \in [\mu_\infty, \bar{\mu}_1]$; the iterated operator $(\Delta_g^m \circ S_\mu)^2$ restricted to the interval $I_{S_\mu}^*$ is simply written

$$(\Delta_g^m \circ S_\mu)^2|_{I_{S_\mu}^*} = \Delta_g^m \circ S_\mu|_{I_{S_\mu}^{1,1}} \circ \Delta_g^m \circ S_\mu|_{I_{S_\mu}^*} \tag{7}$$

to emphasize that at the second application of S_μ only the restriction of the local map to $I_{S_\mu}^{1,1}$ is involved. This is an essential remark, because $I_{S_\mu}^{1,1} \subset [0, 1]$ hence,

$$S_\mu |_{I_{S_\mu}^{1,1}}(X) = 1 - \mu X$$

is *linear*,⁵ and consequently the operator

$$\mathbf{S}_\mu |_{\mathbf{I}_{S_\mu}^{1,1}}(\mathbf{X}) = \mathbf{1} - \mu \mathbf{X}$$

commutes with Δ_g^m :

$$\Delta_g^m \circ \mathbf{S}_\mu |_{\mathbf{I}_{S_\mu}^{1,1}} = \mathbf{S}_\mu |_{\mathbf{I}_{S_\mu}^{1,1}} \circ \Delta_g^m \tag{8}$$

This essential remark permits to write

$$(\Delta_g^m \circ \mathbf{S}_\mu)^2 |_{\mathbf{I}_{S_\mu}^*} = \Delta_g^{2m} \circ \mathbf{S}_\mu^2 |_{\mathbf{I}_{S_\mu}^*} \tag{9}$$

where the iterated operator is expressed also in the form of coupled maps evolving under a iterated local map S_μ^2 and with a longer-range coupling.

Recalling now the centered RG (5) for the local map and linearity of h_{S_μ} , it comes

$$(\Delta_g^m \circ \mathbf{S}_\mu)^2 |_{\mathbf{I}_{S_\mu}^*} = \mathbf{h}_{S_\mu}^{-1} \circ \Delta_g^{2m} \circ \mathbf{S}_{\mu^2} \circ \mathbf{h}_{S_\mu} \tag{10}$$

This relation states that in the two-band regime, the dynamics under an operator $\Delta_g^m \circ \mathbf{S}_\mu$ observed every other timestep is equivalent (conjugate) to another coupled system, $\Delta_g^{m'} \circ \mathbf{S}_{\mu'}$, with a longer-range coupling $m' = 2m$, and parameter value $\mu' = \mu^2$. It is an *exact* RG equation for coupled tent maps in the space of parameters (μ, m) .

In the case of globally coupled maps ($d = \infty$), iterating the coupling amounts to increasing the coupling strength:

$$\Delta_g^m = \Delta_{1-(1-g)^m} \tag{11}$$

therefore the RG operates in the parameter space (μ, g) and $g' = 1 - (1 - g)^2$. However, this is not true in the general case, and certainly not for

⁵ In other words, $0 \notin I_{S_\mu}^{1,1}$ precisely because the “central” band is $I_{S_\mu}^{1,0} \ni 0$ and $I_{S_\mu}^{1,0} \cap I_{S_\mu}^{1,1} = \emptyset$ and 0 is the point of non-linearity of the map.

CMLs: previous attempts to derive a RG for CMLs were looking towards a RG in this parameter space (μ, g) . The calculation above shows that the RG is naturally written in the space (μ, m) .

In the case of the continuous field operator Δ_λ^∞ , the RG can be derived either by performing a similar calculation or taking the continuous limit ($m \rightarrow \infty$ and $\|\vec{e}\| \propto 1/\sqrt{m} \rightarrow 0$) in Eq. (10):

$$(\Delta_\lambda^\infty \circ \mathbf{S}_\mu)^2 |_{\mathbf{I}_{S_\mu}^*} = \mathbf{h}_{S_\mu}^{-1} \circ \Delta_\lambda^\infty \circ \sqrt{2} \circ \mathbf{S}_{\mu^2} \circ \mathbf{h}_{S_\mu} \quad (12)$$

In this case, it operates in the parameter space (μ, λ) and maps λ onto $\lambda' = \lambda \sqrt{2}$.

4.2.2. Noncentered RG. A RG equation can also be derived on the band $\mathbf{I}_{S_\mu}^{1,1}$. However, if the operator $(\Delta_g^m \circ \mathbf{S}_\mu)^2$ is restricted to this band, the commutation (8) leads to $\Delta_g^m \circ (\mathbf{S}_\mu)^2 \circ \Delta_g^m$. It is more appropriate in this case to consider the operator $(\mathbf{S}_\mu \circ \Delta_g^m)^2$ which can be viewed as a coupled system observed just after the application of the map and not just after the coupling step. This does not change the dynamics of the mean M^t while the pdf are compared at intermediate time steps. For these operators the commutation yields:

$$(\mathbf{S}_\mu \circ \Delta_g^m)^2 |_{\mathbf{I}_{S_\mu}^{1,1}} = \mathbf{S}_\mu^2 \circ \Delta_g^{2m} |_{\mathbf{I}_{S_\mu}^{1,1}} \quad (13)$$

Recalling the RG (6) for the local map and linearity of the transformation h'_μ , it comes

$$(\mathbf{S}_\mu \circ \Delta_g^m)^2 |_{\mathbf{I}_{S_\mu}^{1,1}} = \mathbf{h}'_{S_\mu}{}^{-1} \circ \mathbf{S}_{\mu^2} \circ \Delta_g^{2m} \circ \mathbf{h}'_{S_\mu} \quad (14)$$

It is worth noting that the RG does not take the same form on both bands. Previous approaches relied on a commutation between the operators Δ_g and \mathbf{S}_μ under assumptions of weak coupling or as a perturbation approach of a synchronized state, disregarding the properties of the bands of the local map.⁽⁹⁾ Therefore they could not distinguish the bands on which it is possible to make this commutation from the central band where this is certainly not permitted. This distinction leads to the different expressions of the RG.

4.3. Universality

A RG is an powerful tool, and its existence for coupled maps has numerous consequences. We now describe some of these consequences.

4.3.1. Validity. Universality emerges from the group structure which stems from the conjugacy between coupled dynamics and their iterates. Consequently, the validity of universality properties holds if one can insure that this approach can be iterated: in the case of coupled maps this requires that the system reaches banded states of increasing order when $\mu \rightarrow \mu_\infty$. Although this can be guaranteed by an appropriate choice of initial conditions, e.g., restricting initial values to smaller and smaller intervals,⁶ this is not satisfactory in all generality and may appear as a strong impediment to the applicability of a RG approach to coupled maps. In fact, the RG itself provides a simple answer to this difficulty.

Let us first recall that the RG equation (10) relies on the single assumption that the system is in a BS1 for some $\mu \in [\mu_\infty, \bar{\mu}_1]$. Whenever $g > g_e^1(\mu, m)$ such a BS1 is reached from the most general initial conditions under the discrete-space dynamics $\Delta_g^m \circ \mathbf{S}_\mu$.

Consider now that the system is in a BS1 for some appropriate value of the parameter μ and for any g : applying the RG relation (10) establishes the conjugacy between $(\Delta_g^m \circ \mathbf{S}_\mu)^2 |_{\mathbf{I}_{S_\mu}^*}$ and $\Delta_g^{2m} \circ \mathbf{S}_{\mu^2}$. Suppose now that, in fact, $\mu \in [\mu_\infty, \bar{\mu}_2]$, i.e., $\mu^2 \in [\mu_\infty, \bar{\mu}_1]$: the system $\Delta_g^{2m} \circ \mathbf{S}_{\mu^2}$ reaches a BS1 whenever $g > g_e^1(\mu^2, 2m)$. This BS1 is equivalent to a BS2 for $\Delta_g^m \circ \mathbf{S}_\mu$, which is reached whenever $g > g_e^2(\mu, m)$. Thus,

$$g_e^2(\mu, m) = g_e^1(\mu^2, 2m)$$

which expresses the threshold $g_e^2(\mu, m)$ in terms of $g_e^1(\mu, m)$ by use of the RG. This argument is easily generalized to any n . Iterated, it provides a complete description of the different thresholds g_e^n :

$$g_e^n(\mu, m) = g_e^1(\mu^{2^{n-1}}, 2^{n-1}m)$$

In particular, since all $g_e^1(\mu, m)$ have a maximal value $g_e^1(m) = g_e^1(\bar{\mu}_1, m)$ for any fixed m , and using the fact that $g_e^n(\mu, m)$ decreases with m , we have, for all n and μ , $g_e^n(\mu, m) \leq g_e^1(m)$. Consequently, for any given m and $g > g_e^1(m)$, independently of initial conditions, the RG can be applied at all orders, and an infinite cascade of BSs is observed when $\mu \rightarrow \mu_\infty$. In particular, the maximal value of all $g_e^1(m)$ is $g_e^1 = g_e^1(1)$. Moreover, since $g_e^1(\mu, m) \rightarrow 0$ when $m \rightarrow \infty$, $g_e^1(\infty) = 0$ in the case of the continuous limit and a BS of maximal order is always reached.

Consider now some $g < g_e^1(m)$: since $g_e^1(\mu, m) \rightarrow 0$ when $\mu \rightarrow \mu_\infty$ (see Fig. 5), there exists a value $\mu_e^1(g, m)$ of the parameter μ for which

$$g_e^1(\mu_e^1(g, m), m) = g$$

⁶ Such initial conditions were used in ref. 10.

Since $g_e^1(\mu, m)$ is a increasing function of μ , a BS1 is reached by the system $\Delta_g^m \circ \mathbf{S}_\mu$ for all $\mu < \mu_e^1(g, m)$. The same can be said of any critical curve $g_e^n(\mu, m)$ since all $g_e^n(\mu, m) \rightarrow 0$: there exists a value $\mu_e^n(g, m)$ such that $g = g_e^n(\mu_e^n(g, m), m)$. Below $\mu_e^n(g, m)$, a BS n is reached starting from any BS $(n - 1)$. Therefore, below

$$\mu_e^{n*}(g, m) = \min_{n' \leq n} \mu_e^{n'}(g, m)$$

a BS n is reached from any initial condition. In other words, for any given $n > 0$, when $\mu \rightarrow \mu_\infty$, there always exists some μ sufficiently close to μ_∞ to ensure that a BS n is reached. When μ decreases, the system passes first through regions of multistability, but after having crossed the maximal curve $g_e^{n*}(\mu, m)$, it undergoes a full cascade of banded states. These results establish recursively the relevance of the RG approach in all circumstances.

4.3.2. Scaling An immediate consequence of the RG equation (10) is that CML $\Delta_g \circ \mathbf{S}_{\bar{\mu}_1}$ in a banded state at $\bar{\mu}_1$ corresponds to the CML $\Delta_g^2 \circ \mathbf{S}_{\bar{\mu}_0}$ at $\bar{\mu}_0$. More precisely, in a BS1, the behavior of $\Delta_g \circ \mathbf{S}_{\bar{\mu}_1}$ considered every other timestep (when the system lies on the central band) is equivalent to that of CML $\Delta_g^2 \circ \mathbf{S}_{\bar{\mu}_0}$ considered every timestep. Figure 7(b) displays pdf p^t observed in the period-2 regime for a two-dimensional lattice of coupled tent maps. The pdf on the left lies on the central band, and, transformed by the RG, it collapses with the pdf of Fig. 1(b) corresponding to the fixed-point regime for $m = 2$ at $\bar{\mu}_0$.

The same comparison can be performed at all points $\bar{\mu}_n$ for $\Delta_g \circ \mathbf{S}_{\bar{\mu}_n}$ and $\Delta_g^{2^n} \circ \mathbf{S}_{\bar{\mu}_0}$ at $\bar{\mu}_0$. Since in two-dimensional lattices, for $\mu = \bar{\mu}_0$, a fixed-point regime is reached for all m , a period-2 n is reached at every $\bar{\mu}_n$. In the case of three-dimensional lattices (see Fig. 8), a period-2 collective regime is reached for all m at $\bar{\mu}_0$: consequently, period-2 $^{n+1}$ is reached at every band splitting point $\bar{\mu}_n$.

The RG does not predict the behavior displayed by $\Delta_g^m \circ \mathbf{S}_\mu$ on the interval $[\bar{\mu}_1, \bar{\mu}_0]$; however, it relates the behavior of these systems on all other intervals $[\bar{\mu}_{n+1}, \bar{\mu}_n]$ of the parameter μ to the behavior observed on $[\bar{\mu}_1, \bar{\mu}_0]$. This approach is valid whatever the space dimension and the regimes observed for $\mu \in [\bar{\mu}_1, \bar{\mu}_0]$ (fixed-point, periodic, quasi-periodic,...). In higher dimensions, the behavior displayed $\mu \in [\bar{\mu}_1, \bar{\mu}_0]$ can change qualitatively for different (small) values of m , and there is no numerical evidence of what is the behavior displayed in the continuous limit. In these cases, the behavior observed on small- n bands also show qualitative

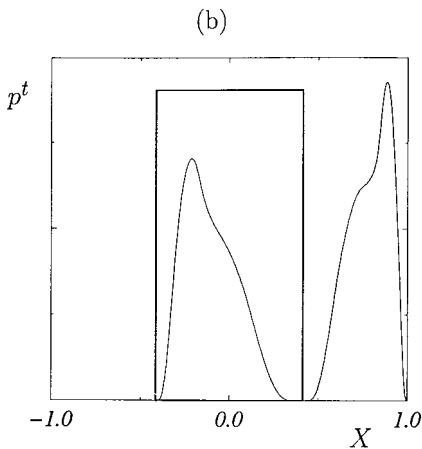
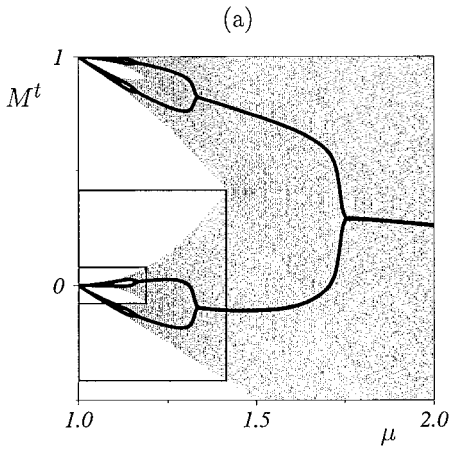


Fig. 7. Democratically-coupled ($g=0.2$) tent maps on a $d=2$ lattice of linear size $L=2048$ with periodic boundary conditions: (a) bifurcation diagram of $M^t = \langle \mathbf{X} \rangle^t$ (filled circles) superimposed on that of the local map S_μ (small dots). The $[\mu_\infty, \bar{\mu}_1] \otimes I_{\bar{\mu}_1}^1$ and $[\mu_\infty, \bar{\mu}_2] \otimes I_{\bar{\mu}_2}^2$ regions are shown. For coupled tent maps, these regions transformed by the RG coincide with the bifurcation diagrams of $\Delta_g^2 \circ S_\mu$ and $\Delta_g^4 \circ S_\mu$, themselves indistinguishable from the whole figure. (b): period-2 collective cycle at $\mu = \bar{\mu}_1$ for $m=1$; the distribution in the rectangle (even time steps) is transformed exactly by the RG onto that for $m=2$ at $\mu=2$ displayed on Fig. 1(b).

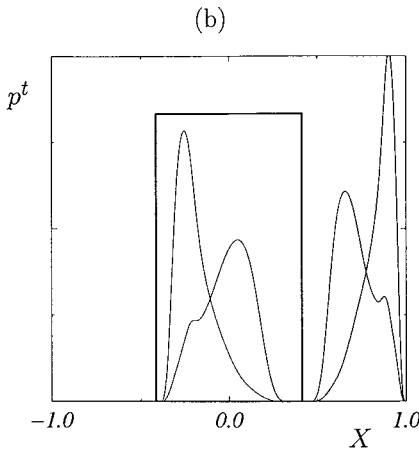
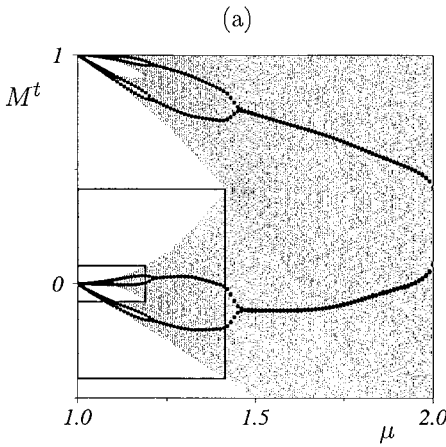


Fig. 8. Democratically-coupled ($g=1/7$) tent maps on a $d=3$ lattice of linear size $L=128$ with periodic boundary conditions: (a) bifurcation diagram of $M^t = \langle \mathbf{X} \rangle^t$ (filled circles) superimposed on that of the local map S_μ (small dots). The $[\mu_\infty, \bar{\mu}_1] \otimes I_{\bar{\mu}_1}^1$ and $[\mu_\infty, \bar{\mu}_2] \otimes I_{\bar{\mu}_2}^2$ regions are shown. For coupled tent maps, these regions transformed by the RG coincide with the bifurcation diagrams of $\Delta_g^2 \circ S_\mu$ and $\Delta_g^4 \circ S_\mu$, themselves indistinguishable from the whole figure. (b): period-4 collective cycle at $\mu = \bar{\mu}_1$ for $m=1$; the distribution in the rectangle (even time steps) is transformed exactly by the RG onto that for $m=2$ at $\mu=2$ displayed on Fig. 2(b).

changes other than the period-doubling implied by the RG. However, in any case, the RG implies that there exists an infinite cascade of “period-doubling” phase transitions for the collective behavior of these CMLs (the term “period-doubling” being understood in a broad sense).

In the space-continuous limit governed by $\Delta_\lambda^\infty \circ \mathbf{S}_\mu$, changing λ amounts to a mere reseating of space: the system is invariant under the symmetry $\lambda \rightarrow \alpha\lambda$ and $\bar{r} \rightarrow \alpha\bar{r}$. Therefore, multiplying λ has no non-trivial effect on the collective behavior: quantities like the instantaneous pdf p^t are not affected at all while the correlation functions are simply reseated in space. Therefore, the RG (12) implies that system $(\Delta_\lambda^\infty \circ \mathbf{S}_\mu)^2$ has exactly the same behavior as $\Delta_\lambda^\infty \circ \mathbf{S}_{\mu^2}$, but with all lengthscales multiplied by $\beta = \sqrt{2}$. In particular, the scaling laws displayed by $\Delta_\lambda^\infty \circ \mathbf{S}_\mu$ are those of the local map with plus the divergence of lengthscales ruled by β . The existence of a phase transition point μ_1^c in the interval $[\bar{\mu}_1, \bar{\mu}_0]$ —and there must be one, since the behavior at $\bar{\mu}_1$ has twice the periodicity of the behavior at $\bar{\mu}_0$ —implies, by similarity, the existence of an infinite cascade of phase transition points μ_n^c related by the RG.

In the case of usual discrete-space CMLs, iterating RG equation (5) shows that, near μ_∞ , the system $\Delta_g^m \circ \mathbf{S}_\mu$ is equivalent to a system on $[\bar{\mu}_1, \bar{\mu}_0]$ with a longer-range coupling ($\Delta_g^{2^m} \circ \mathbf{S}_{\mu'}$) i.e., it is closer to a continuous field map. Therefore, the scaling properties of CMLs are in fact governed by Eq. (12) and rely on the existence of a well-defined continuous limit for the collective behavior. In particular, for the sub-harmonic cascades observed in 2 and 3 dimensions, the phase transitions at μ_n^c are critical points of Ising-like phase transitions,⁽¹⁴⁾ characterized by the divergence of the correlation length. The scaling properties observed in the critical region around these points are not expected to depend on the coupling range m . Therefore, the regions around the critical points μ_n^c are expected to all show the same scaling properties, and their values must scale like the band-merging points $\bar{\mu}_n$ i.e., with, in particular, the Feigenbaum constant δ of the local map.

5. RENORMALIZATION GROUP FOR COUPLED UNIMODAL MAPS

Let us now turn to the more general case when the local map is given by Eq. (2) with $\varepsilon > 0$. We first review briefly how the RG applies to these maps, then, using as a guideline the exact calculation performed for the tent map, we study how the RG can be written in the general case of coupled unimodal maps.

5.1. Single Maps

5.1.1. An Example: The Logistic Map. Let us take the example of the logistic map, $S_\mu(X) = 1 - \mu X^2$, and write,

$$S_\mu^2(X) = 1 - \mu + 2\mu^2 X^2 - \mu^3 X^4 \quad (15)$$

in this case, S_μ^2 is a polynomial of order 4. Clearly, if polynomial maps of the form

$$S_\mu(X) = 1 - \mu^{(1)}X^2 - \mu^{(2)}X^4 \dots$$

are considered, with a more general definition for the parameter μ as the sequence $\mu = (\mu^{(1)}, \mu^{(2)}, \dots)$, the RG transformation operates on these sequences μ : like in the case of the tent map (Eq. (5)), it relies on the existence of a conjugacy between S_μ^2 restricted to a band and a map $S_{\mu'}$ for another parameter value μ' .

Keeping only second order terms in the rhs of Eq. (15) provides the simplest approximation of the RG for the logistic map, $X' = X/(1 - \mu)$ and $\mu' = 2\mu^2(1 - \mu)$ which allows for an estimation of the Feigenbaum constants.⁽⁶⁾

5.1.2. Doubling Transformation. In order to tackle the general case of coupled unimodal maps, we now adopt a more formal point of view on the RG following Collet and Eckmann.⁽¹⁾

Let us denote Ω the space of symmetric, unimodal maps S of the interval $[-1, 1]$ with the *normalization condition* that the maximum (reached for $X=0$) equals 1. For a given map $S \in \Omega$, the bounds of the invariant intervals are the iterates of $X=0$. Let us define,

$$a = -S(1), \quad b = S(a) \quad \text{and} \quad c = S(b)$$

The map S has two bands whenever $0 < a \leq b$ and $c \in I_S^* = [-a, a]$, because the intervals $I_S^{1,0} = [-a, c]$ and $I_S^{1,1} = [b, 1]$ are then exchanged by S , and $I_S^{1,0} \subset I_S^*$. The RG stems from the observation that I_S^* is stable by S^2 , and the map $-S^2$ restricted to I_S^* is again unimodal with a maximum at $X=0$. An appropriate linear change of variables transforms $S^2|_{I_S^*}$ into a normalized unimodal map $T[S] \in \Omega$:

$$S^2|_{I_S^*} = h_S^{-1} \circ T[S] \circ h_S$$

with $h_S(X) = -X/a$. The *doubling transformation* T operates in the space Ω of such maps and the geometric properties of the operator T as a dynamical system acting in Ω determines the universal properties of the local map.⁽⁴⁾ In the case of the tent map, $T[S_\mu] = S_{\mu^2}$.

Let us recall the main results of this approach. Transformation T has a fixed-point Φ and the derivative of T at the point Φ has a simple eigenvalue which is larger than one, which turns out to be the bifurcation velocity, δ . This fixed point verifies the relation $\Phi(X) = -\alpha\Phi \circ \Phi(-X/\alpha)$ which defines the *reduction parameter* $\alpha = -1/\Phi(1)$, characterizing the shrinking of the bands near μ_∞ . The unstable manifold W_u of T is one-dimensional, and the stable manifold W_s has codimension-one.

Let us denote Σ_a the codimension-one surface $\Sigma_a = \{S : S(1) = -a\}$, and Φ_a^* the intersection of W_u with Σ_a . The inverse images of a surface Σ_a by the doubling transformation are denoted,

$$\Sigma_a^{(n)} = T^{-n}[\Sigma_a]$$

and $\Sigma_a^{(0)} = \Sigma_a$. When T^{-1} is iterated, these surfaces accumulate to the stable manifold at the transversal rate δ^{-1} .

A family of maps $\mu \rightarrow S_\mu$ can be regarded as a curve which crosses the stable manifold W_s at the point S_{μ_∞} . For the different maps considered, the point $\bar{\mu}_0 = 2$ corresponds to the case when the image set of the map is the whole interval $[-1, 1]$, i.e., $S_{\bar{\mu}_0}(1) = -1$, and therefore by definition, $S_{\bar{\mu}_0} \in \Sigma_1$. The band-splitting points $\bar{\mu}_n$ correspond to the same property for their images: $T^n[S_{\bar{\mu}_n}] \in \Sigma_1$ or equivalently, $S_{\bar{\mu}_n} \in \Sigma_1^{(n)}$. Therefore the maps $S_{\bar{\mu}_n}$ are the intersection of the curve $\mu \rightarrow S_\mu$ with the surfaces $\Sigma_1^{(n)}$. This shows that the points $\bar{\mu}_n$ converge to μ_∞ at the velocity δ . Moreover when $n \rightarrow \infty$, the sequence $T^n[S_{\bar{\mu}_n}]$ converges to the universal map Φ_1^* which lies on the unstable manifold W_u , while the sequence $T^n[S_{\mu_\infty}] \in W_s$ converges to Φ .

5.2. Maps on Phase Space

Let us now turn to the general case of coupled unimodal maps of the form $\Lambda \circ S$. Multivariate maps have been studied in ref. 19, where it is shown in some cases that a doubling transformation can be defined which guarantees the existence of universal properties. However, it is especially relevant to our problem to find a relation between this universality, the extension of the coupling and the universality of the single map.

In the case of coupled tent maps, the derivation of the self-similarity relation (10) relies on the possibility to let the operators Δ and S commute in the expansion (7) of $(\Delta \circ S)^2$. In the general case, the commutation relation (8) does not hold because the local map is not linear on the interval $I_S^{1;1}$; therefore, the iterated operator restricted to a stable interval cannot be written in the same form (linear coupling composed with a local non-linear map). However, the focal map is invertible on $I_S^{1;1}$ precisely because the only point where it is locally non-invertible lies on the central band (by definition). Invertibility guarantees that the operators $\Delta \circ S$ and $S \circ \Delta$ restricted to $I_S^{1;1}$ are conjugate to each other. This conjugacy can be seen as an extension of the notion of commutation.

The invertibility property and the consequent conjugacy are at the core of the existence of a RG in the general case; it allows to write,

$$(\Delta \circ S)^2|_{\mathbf{I}_S^*} = (\Delta \circ S|_{\mathbf{I}_S^{1;1}} \circ \Delta \circ S|_{\mathbf{I}_S^{1;1}^{-1}}) \circ S^2|_{\mathbf{I}_S^*}$$

which resembles usual coupled maps systems with the local map S^2 but with a non-linear transformation in place of the coupling operator. We show in the following that such nonlinear transformations can be viewed as coupling operators. Embedding the usual linearly coupled maps in a larger space to let the coupling stage incorporate some kind of nonlinearity, the procedure sketched here defines a doubling transformation.

To this aim, more general coupled maps are thus considered, of the form $\mathbf{Q} \circ S$, where \mathbf{Q} itself is a nonlinear operator. Both S and \mathbf{Q} being non-linear might seem confusing: the question arises of the uniqueness of such a decomposition. We argue now that given any unimodal map on \mathbf{I} , there is a unique way to write it in the form $\mathbf{Q} \circ S$. This indicates that the nonlinearities of these two operators are of different nature and play different roles, and guarantees that such systems are well defined.

5.2.1. Canonical Representation. Let us define some space \mathbf{Y} of (continuously differentiable) normalized unimodal maps $\mathbf{X} \rightarrow \Psi(\mathbf{X})$ on the phase space $\mathbf{I} = I^{\mathcal{L}}$ (For simplicity the index set \mathcal{L} can be supposed finite). These maps are taken symmetric (for all $\mathbf{X}_{\bar{r}} \rightarrow -\mathbf{X}_{\bar{r}}$), homogeneous and isotropic to respect the symmetries of the index set \mathcal{L} . Partial maps

$$\mathbf{X}_{\bar{r}_2} \rightarrow [\Psi(\mathbf{X})]_{\bar{r}_1}$$

may be defined, for $\mathbf{X}_{\bar{r}_2}$ varying and $\mathbf{X}_{\bar{r}_1}$ fixed for all $\bar{r} \neq \bar{r}_2$ (in particular, if there is no dependence induced by Ψ between the sites \bar{r}_2 and \bar{r}_1 , this map is flat: such maps are considered as a limit case of unimodal maps).

Unimodality of the map Ψ is defined as the unimodality of all partial maps for all $\vec{r}_2, \vec{r}_1 \in \mathcal{L}$; the absolute maximum for Ψ is obtained at the configuration $\mathbf{X} = \mathbf{0}$. and the normalization condition reads

$$\Psi(\mathbf{0}) = 1$$

Let us denote \mathbf{I}_{syn} , the *synchronous manifold*, i.e., the set of configurations where all sites take the same value: $\mathbf{X}_{\vec{r}} = X$, for all $\vec{r} \in \mathcal{L}$. The image of some synchronized state $\mathbf{X} \in \mathbf{I}_{\text{syn}}$ by a unimodal map Ψ is again synchronized because of homogeneity. The common value of all sites in the image lattice $\Psi[\mathbf{X}]$ is denoted $P[\Psi](X)$. Considering all possible values $X \in I$, $P[\Psi]$ is a normalized, symmetric, unimodal map on I : it is called the *reduced map* of Ψ . Note that, in the case of linearly coupled maps, $\Psi = \Delta \circ \mathbf{S}$ the reduced map is necessarily $P[\Delta \circ \mathbf{S}] = S$.

The reduced map is unimodal with its maximum at 0, and therefore it is invertible from the interval $I^+ = [0, 1]$ to $I_{P[\Psi]}^0 = [-a, 1]$ (with $a = -P[\Psi](1)$); thus, the operator $\mathbf{P}[\Psi]$ transforms the interval \mathbf{I}^+ of configuration with only non-negative values to the whole invariant interval \mathbf{I}_{Ψ}^0 , where the dynamics takes place. This allows to define

$$\mathbf{Q}[\Psi] \equiv \Psi \circ (\mathbf{P}[\Psi])^{-1}$$

on \mathbf{I}_{Ψ}^0 , and to write, in all generality,

$$\Psi = \mathbf{Q}[\Psi] \circ \mathbf{P}[\Psi] \tag{16}$$

to emphasize the coupled manlike structure of unimodal maps in the general case. It is equivalent to take the inverse of the reduced map on $\mathbf{I}^- = -\mathbf{I}^+$ due to the symmetry $\mathbf{X} \rightarrow -\mathbf{X}$. If $\Psi = \Delta \circ \mathbf{S}$, then $\mathbf{Q}[\Psi] = \Delta$, $\mathbf{P}[\Psi] = \mathbf{S}$ and the decompositions amounts to the definition of the map.

The reduced map $P[\Psi]$ can be seen as a mean-field version of Ψ : it accounts for the global transformation applied to a site when setting aside the effects of the other variables (precisely, these effects have been canceled out by taking all the sites synchronized). The operator $\mathbf{Q}[\Psi]$ accounts for the effects of other sites added to this mean-field transformation. It contains no local evolution by itself (its reduced map is the identity) or equivalently, it admits all synchronized states $\mathbf{X} \in \mathbf{I}_{\text{syn}}$ for fixed points. In this sense, $\mathbf{Q}[\Psi]$ is a pure coupling operator, although it is not linear in general.

For any given local map $S \in \Omega$, \mathbf{S} is an uncoupled map on \mathbf{I} . Let us denote Ω the space of such uncoupled maps. The canonical decomposition presented above shows that any map $\Psi \in \Upsilon$ can be written as the composition of some $\mathbf{S} \in \Omega$ with a ‘‘coupling’’ operator. This property can be

written formally as $\mathbf{Y} = \mathbf{Y}' \circ \mathbf{\Omega}$ where \mathbf{Y}' denotes the space of coupling operators. Now, the definition of \mathbf{Y} should be completed by some assumptions, and clearly, these assumptions concern in fact the space \mathbf{Y}' .

Although the coupling operator $\mathbf{Q}[\mathbf{\Psi}]$ already appears as a complicated object, this decomposition shows that under general assumption, there is a unique way of defining a coupled map form for $\mathbf{\Psi}$, and in particular a unique possible local map.

5.2.2. Nonlinear Coupling Operators. We consider coupled map dynamics of the form $\mathbf{\Psi} = \mathbf{Q} \circ \mathbf{S}$, where $\mathbf{Q} \in \mathbf{Y}'$ is taken regular so that the differentiability of $\mathbf{\Psi}$ is determined solely by the local map. The tangent operator for $\mathbf{\Psi}$ is defined by the functional derivative,

$$\frac{\delta \mathbf{\Psi}[\mathbf{X}]_{\bar{r}_1}}{\delta \mathbf{X}_{\bar{r}_2}} = \frac{\delta \mathbf{Q}[\mathbf{X}]_{\bar{r}_1}}{\delta \mathbf{X}_{\bar{r}_2}} S'(\mathbf{X}_{\bar{r}_2})$$

and the form of $\mathbf{\Psi}$ near a maximum is naturally characterized by the exponent ε of the local map as defined by (2).

Other requirements (analogous to properties (1)–(3)) for $\mathbf{\Psi}$ concern the operator $\mathbf{Q} \in \mathbf{Y}'$. Roughly speaking, these properties should insure that \mathbf{Q} behaves as expected from a diffusive coupling operator (DCO) in the most general case: basically, \mathbf{Q} should drive all configurations towards the synchronous manifold, and make all volumes in phase space shrink to the line \mathbf{I}_{syn} . In the case where the coupling operator $\mathbf{Q} = \mathbf{\Delta}$ is linear, properties (1)–(3) are expressed via the kernel

$$\mathcal{D}(\bar{r}_1 - \bar{r}_2) = \frac{\delta \mathbf{\Delta}[\mathbf{X}]_{\bar{r}_1}}{\delta \mathbf{X}_{\bar{r}_2}}$$

which is constant over \mathbf{I} and only depends on the difference $\bar{r}_1 - \bar{r}_2$. For nonlinear couplings, these properties should be reinterpreted in terms of the tangent operator $\delta \mathbf{Q} / \delta \mathbf{X}$.

However, the nonlinear DCOs that are relevant to our problem can be given a simple description. Given a linear diffusive transformation $\mathbf{\Delta}$ with a kernel \mathcal{D} and a coupling length λ , let us consider the operator $\mathbf{Q} = \mathbf{h}^{-1} \circ \mathbf{\Delta} \circ \mathbf{h}$ where h is some smooth change of variables. This operator is conjugate to $\mathbf{\Delta}$ and therefore has an action on phase space which resembles that of a linear DCO. It is homogeneous and accounts for the same lattice symmetries as $\mathbf{\Delta}$; it drives all configurations towards the synchronous manifold. Since h does not induce any correlation between sites (it is purely local), the interaction between sites is completely governed by $\mathbf{\Delta}$. In

particular, the asymptotic (long time) behavior under \mathbf{Q} is determined via $\mathbf{Q}^n = \mathbf{h}^{-1} \circ \Delta^n \circ \mathbf{h}$, and is completely characterized by Δ .⁷

Finally, the composition of such nonlinear diffusive coupling operators is also a diffusive coupling operator since it is nothing else than a (possibly complicated) way to drive a system towards complete synchronization. Such an operator is in general written as

$$\mathbf{Q} = \mathbf{h}_1^{-1} \circ \Delta_1 \circ \mathbf{h}_1 \circ \dots \circ \mathbf{h}_N^{-1} \circ \Delta_N \circ \mathbf{h}_N$$

for some invertible h_i 's and linear couplings Δ_i 's. It means that when \mathbf{Q} is applied, the system is driven towards synchronization by following the Δ_i 's in different systems of coordinates. In particular, the tangent operator of \mathbf{Q} on \mathbf{I}_{syn} is $\Delta_1 \circ \dots \circ \Delta_N$, which defines uniquely the diffusion constant by $\lambda^2 = \sum_i \lambda_i^2$. By construction, the space \mathbf{Y}' of such operators is invariant by composition (which adds up the diffusion constants) and by applying some change of variable (which keeps the diffusion constant invariant).

It is essential to note that all intervals are stable by all $\mathbf{Q} \in \mathbf{Y}'$, while all volumes shrink. These operators drive all configurations to the synchronous manifold and they are characterized by their tangent operator at \mathbf{I}_{syn} which accounts for the strength of the coupling and its spatial extension.

5.3. Doubling Transformation

5.3.1. Definition. The application of the doubling transformation to some map $\Psi = \mathbf{Q} \circ \mathbf{S} \in \mathbf{Y}$ is now straightforward. When the reduced map

⁷ In fact, the derivative of \mathbf{Q} at any configuration \mathbf{X} reads

$$\frac{\delta \mathbf{Q}[\mathbf{X}]_{\bar{r}_1}}{\delta \mathbf{X}_{\bar{r}_2}} = \frac{h'(\mathbf{X}_{\bar{r}_2})}{h'([\mathbf{h}^{-1} \circ \Delta \circ \mathbf{h}(\mathbf{X})]_{\bar{r}_1})} \mathcal{D}(\bar{r}_1 - \bar{r}_2)$$

and depends on \mathbf{X} , although it is constant on \mathbf{I}_{syn} where it is equal to \mathcal{D} . The symmetry \bar{r}_1, \bar{r}_2 , and the invariance by translation are not respected by this operator, by they are recovered by considering its spatial average $\langle \delta \mathbf{Q} / \delta \mathbf{X} \rangle$. This tangent operator accounts for the dependence of an image site on its antecedents. In all cases, $\delta \mathbf{Q} / \delta \mathbf{X}$ is non-negative since h' does not change sign, and the kernel \mathcal{D} is non-negative. The range of this dependence is measured on $\delta \mathbf{Q} / \delta \mathbf{X}$ by a quantity of the form

$$\int (\bar{r}_1 - \bar{r}_2)^2 \frac{\delta \mathbf{Q}[\mathbf{X}]_{\bar{r}_1}}{\delta \mathbf{X}_{\bar{r}_2}} d\bar{r}_1 d\bar{r}_2 = \int \bar{\rho}^2 \left\langle \frac{\delta \mathbf{Q}}{\delta \mathbf{X}} \right\rangle (\bar{\rho}) d\bar{\rho}$$

which remains bounded provided that $|h'|$ verifies $m \leq |h'| \leq M$ for some $M, m > 0$. The assumption on bounds for $|h'|$ is stronger than just invertibility. It insures that the nonlinear coupling operator works in an normal diffusive manner at all points in phase space. It will be always verified in this work.

is in a two-band regime, it exchanges the intervals $I_S^* = [-a, a]$ and $I_S^{1,1} = [b, 1]$. The coupling operator \mathbf{Q} is nonlinear ($\in \mathbf{Y}'$) and keeps intervals invariant: it guarantees that the two disjoint intervals $\mathbf{I}_S^* = [-a, a]^{\mathcal{L}}$ and $\mathbf{I}_S^{1,1} = [b, 1]^{\mathcal{L}}$ are exchanged by Ψ and stable by Ψ^2 . Thus Ψ^2 can be restricted to \mathbf{I}_S^* and reads,

$$\Psi^2|_{\mathbf{I}_S^*} = \mathbf{Q} \circ \mathbf{S}|_{\mathbf{I}_S^{1,1}} \circ \mathbf{Q} \circ \mathbf{S}|_{\mathbf{I}_S^*}$$

Considering Ψ^2 on \mathbf{I}_{syn} shows that its reduced map is S^2 and, using the invertibility of S on $\mathbf{I}_S^{1,1}$, it comes

$$\Psi^2|_{\mathbf{I}_S^*} = (\mathbf{Q} \circ \mathbf{S}|_{\mathbf{I}_S^{1,1}} \circ \mathbf{Q} \circ \mathbf{S}|_{\mathbf{I}_S^{1,1}}^{-1}) \circ \mathbf{S}^2|_{\mathbf{I}_S^*}$$

Applying the linear change of variable $\mathbf{h}_S(\mathbf{X}) = -\mathbf{X}/a$ yields

$$\Psi^2|_{\mathbf{I}_S^*} = \mathbf{h}_S^{-1} \circ \Theta[\Psi] \circ \mathbf{h}_S$$

which defines the doubling transformation in \mathbf{Y} :

$$\Theta[\Psi] \equiv \Theta'_S[\mathbf{Q}] \circ \mathbf{T}[\mathbf{S}] \quad (17)$$

where $\mathbf{T}[\mathbf{S}]$ denotes the uncoupled map which transforms each local variable by $T[S]$ while

$$\Theta'_S[\mathbf{Q}] \equiv \mathbf{h}_S \circ (\mathbf{Q} \circ (\mathbf{S}|_{\mathbf{I}_S^{1,1}} \circ \mathbf{Q} \circ \mathbf{S}|_{\mathbf{I}_S^{1,1}}^{-1})) \circ \mathbf{h}_S^{-1} \quad (18)$$

defines the action of the doubling transformation on the space \mathbf{Y}' of non-linear coupling operators.

We have shown that there exists a unique way to define the doubling transformation, and that it respects, in any case, the RG of the local map. This strong property stems from the uniqueness of the reduced map, for a given unimodal map on the phase space.

When the doubling transformation is applied to map Ψ , its reduced map is transformed by the local doubling transformation T on Ω (Θ and \mathbf{P} commute) and when Ψ follows the flow of Θ in \mathbf{Y} , $\mathbf{P}[\Psi]$ follows the flow of T in Ω . Taking the local map in the stable (resp. unstable) manifold of the local RG shows that the manifolds $\mathbf{Y}' \circ \mathbf{W}_s \subset \mathbf{Y}$ (resp. $\mathbf{Y}' \circ \mathbf{W}_u$) are invariant by Θ .

Similarly, the univoque definition of a diffusion constant for the DCO that we consider, shows that, under the doubling transformation, the diffusion constant doubles i.e., the coupling length is multiplied by $\beta = \sqrt{2}$. This property was already found for coupled tent maps, and appears to be

directly related to the “synchronously updated” form of the evolution operator. It must also be accompanied by a decay of the lattice mesh size, $\|\vec{e}\|$: the lattice converges to a continuous limit.

However, the precise action of the doubling transformation on DCOs in the space \mathbf{Y}' is complicated and “coupled” to the local RG. Iterating (18) shows that Θ'^n involves the different iterates of the local map under T . In some sense, the dynamical operator Θ' depends on the “time” n when iterated. However, when the local map, iterated by the RG, converges to some universal map, the operator Θ' also converges and the existence of some limit behavior for the coupling operator arises from the properties of this asymptotic Θ' .

Let us consider the case when the local map is the fixed point Φ :

$$\Theta[\mathbf{Q} \circ \Phi] \equiv \Theta'_{\Phi}[\mathbf{Q}] \circ \Phi$$

and accompany the doubling transformation with the rescaling $\|\vec{e}\| \rightarrow \|\vec{e}\|/\beta$. Under this transformation, the coupling length λ is unchanged. It is an open question to determine whether there exists, like in the case of coupled tent maps, a universal operator $\mathbf{Q}_{\lambda}^{\infty}$ verifying the fixed point relation:

$$\mathbf{h}_{\Phi} \circ (\mathbf{Q}_{\lambda}^{\infty} \circ (\Phi|_{\mathbf{I}_{\Phi}^{1,1}} \circ \mathbf{Q}_{\lambda}^{\infty} \circ \Phi|_{\mathbf{I}_{\Phi}^{-1,1}})) \circ \mathbf{h}_{\Phi}^{-1} = \mathbf{Q}_{\lambda\beta}^{\infty}$$

In the case of linearly coupled tent maps, this equation reduces to the equality,

$$(\mathbf{Q}_{\lambda}^{\infty})^2 = \mathbf{Q}_{\lambda\beta}^{\infty}$$

which is verified by $\Delta_{\lambda}^{\infty}$. But, in general, the existence of such a limit is not proven.

5.3.2. Qualitative Universality

Limits of NTS. The application of the doubling transformation relies on the assumption that the system is in a BS. The RG can be iterated independently of initial conditions provided that the system reaches BSs of increasing order when $\mu \rightarrow \mu_{\infty}$. Like in the case of coupled tent maps, the generality of this approach stems from the observation that taking $\mu \rightarrow \mu_{\infty}$ amounts to a strengthening of the coupling and guarantees that, for sufficiently strong coupling, there is an infinite sub-harmonic cascade of phase transitions. Let us now detail this argument. We consider a lattice of non-linearly coupled maps, $\Psi = \mathbf{Q}_q \circ \mathbf{S}_{\mu}$: this could represent a CML of the form $\Delta_g^m \circ \mathbf{S}$, where the two parameters m and g of the original coupling operator are encoded by the “strength” q .

For $\mu \leq \bar{\mu}_n$, a BS n is reached from almost all initial conditions in a BS($n-1$) whenever the coupling strength is larger than the limit value $g_e^n(\Psi)$. If moreover $\mu \leq \bar{\mu}_{n+1}$, the map $T[S_\mu]$ has 2^n bands, and the system $\Theta[\Psi]$ reaches a BS n for $g > g_e^n(\Theta[\Psi])$: this situation corresponds to a BS($n+1$) in the 2^{n+1} -band regime of S_μ , hence

$$g_e^{n+1}(\Psi) = g_e^n(\Theta[\Psi])$$

Let us denote $\mathbf{Q}_q^{(n)} \circ \mathbf{T}^n[\mathbf{S}_\mu]$ the successive images of $\Psi = \mathbf{Q}_q \circ \mathbf{S}_\mu$ by the doubling transformation. From the definition (18) of doubling transformation Θ' for DCOs, $\mathbf{Q}_q^{(n+1)}$ is a “stronger” coupling than $\mathbf{Q}_q^{(n)}$ in the sense that it makes the volume of the phase space shrink even more. Consequently, for any fixed local map S with at least two bands, the system $\mathbf{Q}_q^{(n)} \circ \mathbf{S}$ reaches banded states more easily with n increasing, hence $g_e^1(\mathbf{Q}_q^{(n)} \circ \mathbf{S})$ decreases with n . Moreover, when $n \rightarrow \infty$, the coupling length diverges at a fixed mesh size (i.e., the ratio $\lambda/\|\vec{e}\|$ diverges like β^n) taking $\|\vec{e}\| \propto \beta^{-n}$ shows that for large n , $\mathbf{Q}_q^{(n)}$ corresponded to a coupling operator for a continuous field without even knowing precisely the behavior of $\mathbf{Q}_q^{(n)}$ in this limit. Therefore, the discretization of the lattice disappears, there is no possible pinning of clusters to allow for the co-existence of phases and $g_e^1(\mathbf{Q}_q^{(n)} \circ \mathbf{S})$ is expected to vanish:

$$g_e^1(\mathbf{Q}_q^{(n)} \circ \mathbf{S}) \xrightarrow{n \rightarrow \infty} 0 \quad (19)$$

If the system is considered, e.g., at all $\bar{\mu}_n$, the property (19) added to the fact that the sequence $\mathbf{T}^n[\mathbf{S}_{\bar{\mu}_n}]$ converges to Φ_1^* shows that the sequence

$$g_e^n(\mathbf{Q}_q \circ \mathbf{S}_{\bar{\mu}_n}) = g_e^1(\mathbf{Q}_q^{(n)} \circ \mathbf{T}^n[\mathbf{S}_{\bar{\mu}_n}])$$

vanishes in the limit $n \rightarrow \infty$; in particular it is bounded above which shows that by an appropriate choice of the coupling strength q , i.e., the strength and/or the extension of the DCO Δ_g^m , the sub-harmonic cascade of banded states is infinite. In this strong-coupling limit, coupled maps exhibit their universal behavior.

Illustration. The RG is illustrated in Fig. 9 on the case of democratically-coupled logistic maps on a 2-dimensional lattice. Period 2^n is observed at the points $\bar{\mu}_n$, i.e., for $\Psi = \Delta_g \circ \mathbf{S}_{\bar{\mu}_n}$: these regimes correspond to fixed points for $\Theta^n[\Delta_g \circ \mathbf{S}_{\bar{\mu}_n}]$. When n increases, the reduced map of these operators follows the local RG and therefore converges to the universal map Φ_1^* .

These distributions were evaluated by the direct simulation of $\Delta_g \circ S_{\bar{\mu}_n}$, and the measure of the pdfs when the system lies on the central band, followed by a simple resealing. These pdfs p_n are displayed on Fig. 9(d) where it is clear that they admit a well-defined limit when $n \rightarrow \infty$. This limit does not necessarily corresponds to the existence of a limit for the coupling operator iterated by Θ' and involving all $T^n[S_{\bar{\mu}_n}]$: it is the macroscopic motion produced by the operators of the form $Q_q^{(n)} \circ \Phi_1^*$ which admit a well-defined limit when $n \rightarrow \infty$.

5.4. Metric Properties

In the case $\Psi = \Delta \circ S_\mu$, for a family of unimodal maps, the bands shrink when the parameter μ approaches μ_∞ . On these bands of decaying width, the local map (which is invertible on each of these bands) can be approximated by its tangent: in this linear approximation, the commutation of operators Δ and S_μ can be performed, thus yielding to the same doubling transformation as for coupled tent maps.

5.4.1. Commuting Doubling Transformation. Let us first define a “commuting” doubling transformation for which the commutation is performed *a priori*:

$$\Theta_c[Q \circ S] \equiv Q^2 \circ T[S] \quad (20)$$

We then intend to compare the transformations Θ and Θ_c near the point μ_∞ . Denoting

$$\Theta_c[\Delta \circ S] \equiv \Theta'_c[\Delta] \circ T[S]$$

and

$$\Theta'_c[\Delta] \equiv \Delta^2$$

allows to separate Θ_c into the local RG transformation T and the spatial RG transformation Θ'_c . This is the same RG as for coupled tent maps. The situation is thus particularly simple: when the commuting doubling transformation is iterated, the coupling converge to the family of universal operators Δ_λ^∞ while the local map follows its own RG flow.

5.4.2. Asymptotic Equivalence. In order to quantify the difference between the actual RG of some unimodal map, and the commuting RG, let us first estimate the commutator

$$[\Delta, S] = \Delta \circ S - S \circ \Delta$$

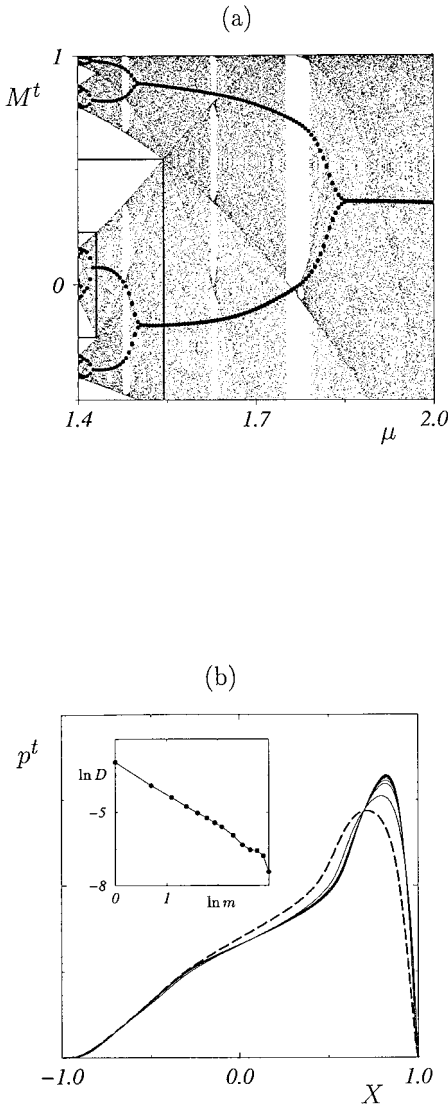


Fig. 9. Two-dimensional lattice of democratically coupled ($g=0.2$) logistic maps. (a): Bifurcation diagram of M^t (circle) compared with the bifurcation diagram of the single logistic map; the $[\mu_\infty, \bar{\mu}_1] \otimes I_{\bar{\mu}_1}^1$ and $[\mu_\infty, \bar{\mu}_2] \otimes I_{\bar{\mu}_2}^2$ regions are shown. (b)–(d): Asymptotic regime for the single-site pdf p^t . (b): stationary state at $\mu=2$ for $1 \leq m \leq 32$; they converge towards the pdf for the continuous limit. (c): period-2 collective cycle at the first band-splitting point $\mu = \bar{\mu}_1$; the distribution in the rectangle corresponds to the times when all sites lie on the central band and is reported on (b) (dashed) after renormalization. (d): Period- 2^n is found at all points $\bar{\mu}_n$ and the normalized pdfs on the central band converge.

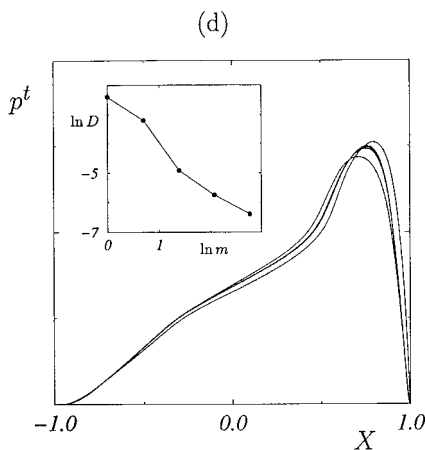
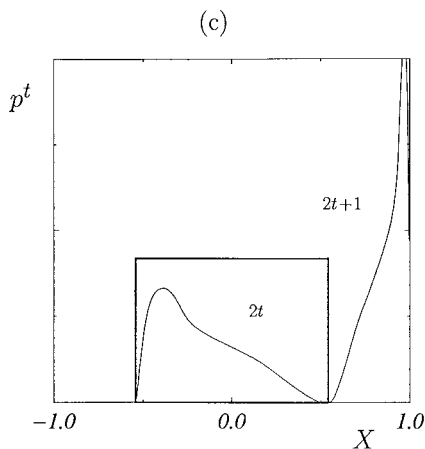


Fig. 9. (Continued)

of Δ and S applied to some configuration \mathbf{X} . For this purpose, each local variable is written

$$\mathbf{X}_F = \langle \mathbf{X} \rangle + \mathbf{x}_F$$

where the field \mathbf{x} has been introduced which measures the local departure from the mean-field $M = \langle \mathbf{X} \rangle$. A Taylor expansion of the local map around M reads,

$$S(\mathbf{X}_F) = S(M) + \mathbf{x}_F S'(M) + \frac{(\mathbf{x}_F)^2}{2} S''(M) + \dots$$

for the configuration \mathbf{X} . Similarly, for $\Delta(\mathbf{X}) = \mathbf{M} + \Delta(\mathbf{x})$, it reads,

$$S([\Delta(\mathbf{X})]_{\bar{r}}) = S(M) + [\Delta(\mathbf{x})]_{\bar{r}} S'(M) + \frac{([\Delta(\mathbf{x})]_{\bar{r}})^2}{2} S''(M) + \dots$$

Applying Δ to the first of these equations, and performing the difference, only the second order terms remain and it comes

$$[\Delta, \mathbf{S}](\mathbf{X}) = \frac{1}{2} [\Delta(\mathbf{x}^2) - [\Delta(\mathbf{x})]^2] S''(M) + \dots$$

If moreover, the histogram of all sites in the configuration \mathbf{X} lies on an interval $I_{\mathbf{X}}$ of width $\eta_{\mathbf{X}}$, the rhs of this equation is dominated by $\eta_{\mathbf{X}}^2 \max_{I_{\mathbf{X}}} |S''|/2$, and

$$\|[\Delta, \mathbf{S}](\mathbf{X})\| = \mathbf{O}(\eta_{\mathbf{X}}^2 \max_{I_{\mathbf{X}}} |S''|)$$

where the norm $\|\mathbf{X}\| = \max X_{\bar{r}}$ has been introduced. This allows to estimate the error made when applying the commuting doubling transformation. When the operator

$$(\Delta \circ \mathbf{S})^2 - \Delta^2 \circ \mathbf{S}^2 = \Delta \circ [\mathbf{S}, \Delta] \circ \mathbf{S}$$

is evaluated on some configuration $\mathbf{X} \in \mathbf{I}_S^*$, the commutator $[\mathbf{S}, \Delta]$ is estimated on the configuration $\mathbf{S}(\mathbf{X})$. If $\mu \rightarrow \mu_{\infty}$, the bands shrink and become small compared to the interval I_S^* : the state $\mathbf{S}(\mathbf{X})$ lies on an interval $I_{\mathbf{S}(\mathbf{X})} \subset I_S^{1,1}$ which is much smaller than the “meta-bands” I_S^* or $I_S^{1,1}$. Denoting η_{μ} the average width of the bands μ , $\eta_{\mu} \rightarrow 0$ when $\mu \rightarrow \mu_{\infty}$. Moreover the second derivative of S which appears in the commutator only involves values in $I_S^{1,1}$, and $\max_{I_S^{1,1}} |S''| = \mathbf{O}(\varepsilon)$. This provides the estimate

$$\|[(\Delta \circ \mathbf{S})^2 - \Delta^2 \circ \mathbf{S}^2](\mathbf{X})\| = \mathbf{O}(\eta_{\mu}^2 \varepsilon)$$

This result should be compared to fluctuations of the local values in the configuration \mathbf{X} itself, measured by $\|\mathbf{x}\| = \|\mathbf{X} - \mathbf{M}\|$ which is of order η_{μ} : it comes,

$$\frac{\|[(\Delta \circ \mathbf{S})^2 - \Delta^2 \circ \mathbf{S}^2](\mathbf{X})\|}{\|\mathbf{X} - \mathbf{M}\|} = \mathbf{O}(\eta_{\mu} \varepsilon)$$

Therefore, after performing the linear change of variables $\mathbf{h}_S \mathbf{X} \rightarrow -\mathbf{X}/a_{\mu}$ ($a_{\mu} = 1 - \mu$), it comes,

$$\frac{\|\Theta[\Delta \circ \mathbf{S}](\mathbf{X}) - \Theta_c[\Delta \circ \mathbf{S}](\mathbf{X})\|}{\|\mathbf{X} - \mathbf{M}\|} = \mathbf{O}(\eta_{\mu} \varepsilon)$$

This means that the perturbation induced by the commutation decays in either one of the two limits $\mu \rightarrow \mu_\infty$ or $\varepsilon \rightarrow 0$. For any fixed ε , Θ and Θ_c are therefore tangent near the stable manifold: hence, the metric properties of the doubling transformation Θ , corresponding to its tangent description near μ_∞ are given by those of the “commuting” doubling transformation.

5.4.3. Scaling Consequences and Universality. The commuting doubling transformation associates the operator $\Delta_g \circ \mathbf{S}_{\bar{\mu}_n}$ to

$$\Theta_c^n[\Delta_g \circ \mathbf{S}_{\bar{\mu}_n}] = \Delta^{2^n} \circ \mathbf{T}^n[\mathbf{S}_{\bar{\mu}_n}]$$

In this case the existence of a limit when $n \rightarrow \infty$ arises directly from the existence of a well-defined collective behavior in the continuous limit and when the local map converges to a universal map: when $n \rightarrow \infty$, the operator $\Theta_c^n[\Delta_g \circ \mathbf{S}_{\bar{\mu}_n}]$ converges to $\Delta_\lambda^\infty \circ \Phi_1^*$.

We studied this convergence numerically from a simulation of $\Delta^{2^n} \circ \mathbf{S}_{\bar{\mu}_n}^{2^n}$ followed by a simple rescaling of the pdfs on the central band. The fixed-point pdfs p_n^c observed for these systems are displayed Fig. 10(a) for n varying from 1 to 32. They are then compared with the universal collective fixed-points p_n obtained from $\Theta^n[\Delta_g \circ \mathbf{S}_{\bar{\mu}_n}]$: p_{32} and p_{32}^c are displayed on Fig. 10(b) and differ by less than one percent. However, these series of pdfs are not expected to have the same limit, and this appears when the distances $D(p_n - p_n^c)$ are plotted versus n (insert of Fig. 10(b)). This excellent agreement indicates that the macroscopic motion induced by the operator $\Theta^n[\Delta_g \circ \mathbf{S}_{\bar{\mu}_n}]$ is essentially dominated by its expression near the synchronous manifold: in this limit, the space is continuous, the profile \mathbf{X}_r is smooth, and the largest weights in the coupling are attributed to the nearest sites.

In the case of the continuous field dynamics, $\Delta_\lambda^\infty \circ \mathbf{S}_\mu$, the commuting doubling transformation (20) reads,

$$\Theta_c[\Delta_\lambda^\infty \circ \mathbf{S}_\mu] = \Delta_{\lambda\sqrt{2}}^\infty \circ \mathbf{T}[\mathbf{S}_\mu] \quad (21)$$

Thanks to the asymptotic equivalence, it characterizes the universal properties of coupled dynamics. In this case, the RG holds in its greatest generality since BSs of maximal order are always reached. Moreover, because λ does not affect the collective behavior of the single-site observables contained in p^t , Eq. (21) is strictly equivalent to the RG equation for the local map for these macroscopic quantities. In particular, the width w of these pdfs therefore scales with the reduction parameter α of the local map: $w \simeq (\mu - \mu_\infty)^\gamma$ with $\gamma = \ln \alpha / \ln \delta$. However, this “normal” behavior of the single-site observables is accompanied by an increase of the coupling

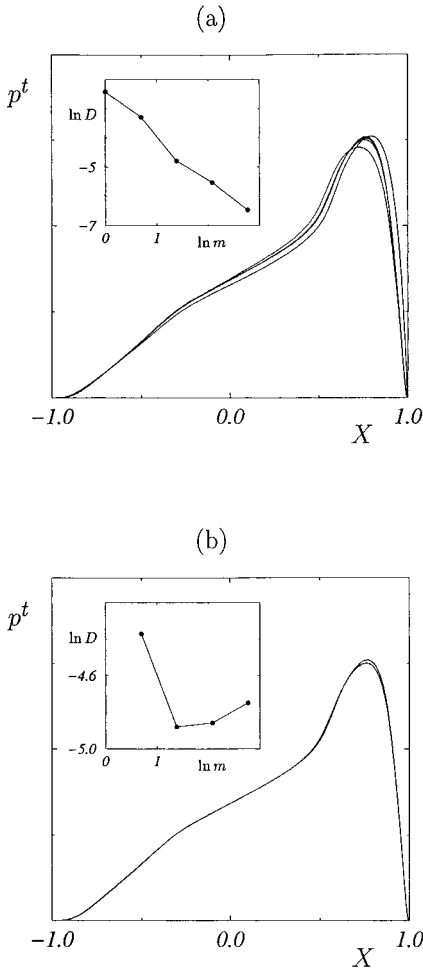


Fig. 10. 2-dimensional lattice of democratically coupled ($g=0.2$) logistic maps. (a): fixed point regimes displayed by the operators $\Theta_c^g[\Delta_g \circ \mathbf{S}_{\bar{\mu}_n}]$. (b) comparison of the universal collective behaviors obtained from the RG and the commuting RG.

length, since it is multiplied by $\beta = \sqrt{2}$ at each period doubling. The same dilatation applies to all length-scales and in particular to the coherence and correlation length: $\xi \simeq (\mu - \mu_\infty)^{\beta'}$ with $\beta' = \ln \beta / \ln \delta$. Let us mention finally that in this continuous limit, the Lyapunov exponents are *not* expected to be related to the coupling length λ , and they all scale like their local counterpart: $A \simeq (\mu - \mu_\infty)^v$ with $v = \ln 2 / \ln \delta$. However, this does not indicate, as claimed in 10 the existence of a relation of the form $\xi \simeq A^{-1/2}$ in all

generality: spatial lengthscales and Lyapunov exponents may vary differently on any interval $[\bar{\mu}_{n+1}, \bar{\mu}_n]$. This is quite obvious at the Ising-like phase transition points μ_n^c observed for $d=2$ and $d=3$, where the correlation length diverges while the largest Lyapunov exponent does not vanish.⁽¹⁴⁾

For large n , if the map is observed, e.g., at the band-splitting points, $\Theta_c^n[\Delta_\lambda^\infty \circ S_{\bar{\mu}_n}]$ is equivalent to the universal coupled system $\Delta_{\lambda\beta^n}^\infty \circ \Phi_1^*$ with a diverging coupling length, while $\Theta_c^n[\Delta_\lambda^\infty \circ S_{\mu_\infty}]$ is equivalent to $\Delta_{\lambda\beta^n}^\infty \circ \Phi$.

These results for the continuous field operator $\Delta_\lambda^\infty \circ S_\mu$ can be immediately translated to the case of discrete (usual) CMLs. In this case, the commuting doubling transformation (20) can be accompanied by a resealing of the lattice mesh size to maintain a constant coupling length λ . This shows that all the scaling properties of the local map are transmitted to the coupled system, with the additional exponent $\beta = \sqrt{2}$ characterizing the divergence of length-scales. Similarly, the shrinking of the widths of the pdfs on the central band is controlled by the exponent α . This provides a complete explanation of the results obtained numerically by van der Water and Bohr.⁽¹⁰⁾

For example, in the case of two- or three-dimensional lattices of coupled tent or logistic maps, the bifurcation points μ_n^c which are Ising-like phase transitions are related to each other by the RG like the band splitting points $\bar{\mu}_n$ and therefore follow the same universal behavior. The convergence $\mu_n^c \rightarrow \mu_\infty$ is characterized by the Feigenbaum constant δ of the local map. For the same reasons, the root mean square of the pdfs p^t shrinks like the widths of the bands. Finally, for large n , operator $\Delta_g^m \circ S_{\bar{\mu}_n}$ is equivalent to the universal operator $\Delta_\lambda^\infty \circ \Phi_1^*$. This is illustrated on Fig. 9 where the asymptotic renormalized pdfs on the central band at the points $\bar{\mu}_n$ are observed to converge.

6. CONCLUSION

Our work has shown how RG equations can be derived for coupled unimodal maps. Like in the case of maps of an interval, this RG relies on the following observation (which holds under some assumptions to be defined more precisely): given a normalized unimodal map Φ on the phase space \mathbf{I} , the iterated map Φ^2 can be restricted to an interval, and, by an appropriate resealing, yields again a normalized unimodal map on \mathbf{I} . The transformation Θ , which associates this unimodal map to Φ , is called the doubling transformation and provides the natural framework for understanding the self-similarity properties of discrete-time spatially-extended dynamical systems.

RG for Banded States. In the case of coupled maps, $\Phi = \Delta_g^m \circ S_\mu$, and the RG equations hold for configurations where all sites lie in the same

band at every timestep (banded-states). The RG relies on the commutation properties of the coupling operator with the local map on bands where the local map is invertible. It takes a simple form when applied to the case of coupled tent maps since,

$$\Theta[\Lambda_g^m \circ S_\mu] = \Lambda_g^{2m} \circ S_{\mu^2}$$

In this case the RG operates directly in the parameter space (μ, m) : $(\mu, m) \rightarrow (\mu^2, 2m)$ where the transformation $\mu \rightarrow \mu^2$ corresponds to the RG for the tent map. This example provides a clear illustration of how the RG acts: the local map is transformed by its own (local) doubling transformation T while the coupling operator is iterated, implying the doubling of the diffusion constant, i.e., a multiplication of the coupling length λ by $\beta = \sqrt{2}$.

The expression of the RG requires more care in the general case of coupled unimodal maps. It leads to embed the usual linearly coupled maps into the wider space \mathbf{Y} of coupled maps of the form $\mathbf{Q} \circ \mathbf{S}$. The DCO \mathbf{Q} may contain some nonlinearities, although it should operate like a linear DCO at least locally in phase space. With this enlarged definition, the doubling transformation operates on \mathbf{Y} and can be specified by its action on the local map and on the DCO. It is striking that, in all cases, the local map S is always transformed by its own (local) doubling transformation T . Meanwhile, the (nonlinear) DCO \mathbf{Q} is transformed into an operator (which resembles \mathbf{Q}^2) with a doubled diffusion constant like in the case of linearly coupled tent maps.

Commuting Doubling Transformation. Two remarks summarize this approach: Firstly, a RG relation can indeed be written in the general case, and it transforms the local map by the RG for maps on an interval. Secondly, the action of this RG on nonlinear DCO resembles the iteration $\mathbf{Q} \rightarrow \mathbf{Q}^2$. This leads to define a commuting doubling transformation Θ_c which is an approximation of the exact RG. It accounts qualitatively for the self-similarity displayed by these systems. Moreover, the property that, near μ_∞ , the bands shrink, allows to show that Θ shares the universal properties of Θ_c .

No Hypothesis on the Behavior on $[\bar{\mu}_1, \bar{\mu}_0]$. The RG approach does not provide any description of the behavior on the interval of parameter $[\bar{\mu}_1, \bar{\mu}_0]$; meanwhile, it does not rely on any assumption about this behavior. This situation is similar, in fact, similar to the case of single maps, where depending on $\mu \in [\bar{\mu}_1, \bar{\mu}_0]$, the system can be ergodic or reach a periodic window. In the case of coupled maps, for a given coupling operator, a given dimension, a given local map and $\mu \in [\bar{\mu}_1, \bar{\mu}_0]$, the collective behavior can be periodic or quasi-periodic, can display some

hysteresis,... and this is not predicted by the RG. However, the RG permits to relate the different regimes on all intervals $[\bar{\mu}_{n+1}, \bar{\mu}_n]$ to the behavior observed on $[\bar{\mu}_1, \bar{\mu}_0]$. Since no assumption is made about the particular collective dynamics in a given band nor about the local state of the lattice, the RG approach is very general and can be applied to CMLs in all dimensions, globally-coupled maps, etc. However, the universal collective behavior reached near μ_∞ is directly related to the continuous limit which remains essentially unexplored in higher dimensions.

Validity. The single requirement needed to apply the doubling transformation is that the system is in a BS. The property that, for strong enough coupling, and from almost initial conditions, the system flows to a BS has been termed non-trivial synchronization (NTS), and is a weaker property than NTCB. However, the requirements on the coupled maps dynamics to insure that NTCB is reached are often not explicit. A usual assumption is that NTCB is achieved for sufficiently strong coupling strengths. Therefore, the study of the necessary conditions for NTS is of great interest since it allows both to state when the RG can be applied to generic asymptotic regimes, and also to shed some light on NTCB. By use of the RG itself, it is possible to show that, when $\mu \rightarrow \mu_\infty$, the coupling operator takes on a wider spatial extension and therefore appears to be stronger compared to the local map. This insures that a coupling operator that guarantees that NTS is reached in a two-band regime, also allows to reach NTS for any number of bands encountered when $\mu \rightarrow \mu_\infty$. Consequently, there must be an infinite sub-harmonic cascade of phase transitions, independently of the particular behavior observed on $[\bar{\mu}_1, \bar{\mu}_0]$.

Scaling Properties. Although the commuting doubling transformation is purely qualitative for the comparison of the regimes on the intervals $[\bar{\mu}_{n+1}, \bar{\mu}_n]$ and $[\bar{\mu}_1, \bar{\mu}_0]$, it becomes exact in the limit $\mu \rightarrow \mu_\infty$, when comparing the regimes on $[\bar{\mu}_{n+1}, \bar{\mu}_n]$ and $[\bar{\mu}_n, \bar{\mu}_{n-1}]$ for $n \rightarrow \infty$. Therefore, it is sufficient to study the universality properties displayed by Θ_c to characterize the universality properties of coupled maps. The commuting doubling transformation has the same simple form as in the case of the coupled tent maps: it associates the properties of the RG for the local map to the convergence of the coupling operator to the continuous limit, Δ_λ^∞ . This insures that the scaling properties of the local map are preserved (this concerns the transition points, the rms of the asymptotic pdfs,...) and that lengthscales are multiplied by $\beta = \sqrt{2}$ at each step.

This work provides the basis of a rigorous approach to RG for coupled map systems. We have shown that the continuous limit plays an essential role since the operator Δ_λ^∞ is universal. We stress that the strong

coupling limit of coupled maps, rather than corresponding to some particular, large value of the parameter g , is reached by considering continuously coupled maps. Thus, any weak-coupling strategy appears irrelevant when trying to account for nontrivial collective behavior.⁽²⁰⁾ Moreover, the continuous limit provides the natural framework within which a “zero temperature” expansion should be carried out and therefore seems to be a key ingredient when trying to understand the emergence of collective motion from local chaos.

REFERENCES

1. P. Collet and J. P. Eckmann, *Iterated Maps of the Interval as Dynamical Systems* (Birkhäuser, Boston, 1980).
2. See, e.g., P. Cvitanović (ed.), *Universality in Chaos*, 2nd ed., (Adam Bilger, Boston, 1989).
3. M. J. Feigenbaum, *J. Stat. Phys.* **19**:25 (1978); **21**:669 (1979); *Physica D* **7**:16 (1983); P. Couillet and J. Tresser, *J. Phys. C* **5**:25 (1978).
4. P. Collet, J. P. Eckmann and O. E. Lanford III, *Commun. Math. Phys.* **76**:211–254 (1980).
5. N. Metropolis, M. L. Stein and P. R. Stein, *J. Comb. Theory A* **15**:25 (1973).
6. B. Derride, A. Gervois, and Y. Pomeau, *J. Phys. A* **12**:269 (1979).
7. See, e.g., K. Kaneko, Ed., *Theory and Applications of Coupled Map Lattices*, (Wiley, New York, 1993), and references therein.
8. S. P. Kuznetsov and A. S. Pikovsky, *Physica D* **19**:384 (1986).
9. For a review, see: S. P. Kuznetsov, in 7 and references therein.
10. W. van der Water and T. Bohr, *Chaos* **3**:747 (1993).
11. A. Lemaître and H. Chaté, *Phys. Rev. Lett.* **80**:5528 (1998).
12. H. Chaté and P. Manneville, *Prog. Theor. Phys.* **87**:1 (1992); *Europhys. Lett.* **17**:291 (1992); H. Chaté and J. Losson, *Physica D* **103**:51 (1997).
13. A. Lemaître and H. Chaté, Phase-ordering and onset of collective behavior in chaotic coupled map lattices, preprint, 1998.
14. P. Marcq, Ph.D. thesis, Université P. & M. Curie (1996); P. Marcq, H. Chaté, and P. Manneville, in preparation.
15. A. Lemaître and H. Chaté, unpublished.
16. A. Lemaître, Ph.D. Dissertation, École Polytechnique, 1998.
17. I. Dornic and C. Godrèche, *J. Phys. A* **31**:5413 (1998), and references therein; D. Stauffer, *J. Phys. A* **27**:5029 (1994).
18. J. P. Crutchfield and B. A. Huberman, *Phys. Lett. A* **77**:407 (1980); J. P. Crutchfield, M. Nauenberg and J. Rudnik, *Phys. Rev. Lett.* **46**:933 (1981).
19. P. Collet, J. P. Eckmann and H. Koch, Period Doubling Bifurcation for Families of Maps on R^n , *Commun. Math. Phys.* **76**:211–254 (1980).
20. See, e.g., J. Bricmont and A. Kupiainen, *Comm. Math. Phys.* **178**:703 (1996); *Physica D* **103**:18 (1997).